

Supporting Information

A series of Isostructural Metal-Organic Frameworks for Enhanced Electro-catalytic Oxygen Evolution Reaction

(Supporting Information: 44 pages including this page)

Pampa Jhariat,^b Abdul Kareem,^{‡b} Priyanka Kumari,^{‡b} Shafeeq Sarfudeen,^b
Premchand Panda,^b Sellappan Senthilkumar,^b and Tamas Panda^{*a,b}

^a *Centre for Clean Environment (CCE), Vellore Institute of Technology, Vellore Campus, Katpadi, Vellore 632014,*

^b *Department of Chemistry, School of Advanced Science, Vellore Institute of Technology, Vellore-, 632014, Tamil Nadu, India.*

E-mail: tamaskumpanda@vit.ac.in

CONTENT

Section S1. General Information	S3
Section S2. Experimental procedure	S4-S6
Section S3. Characterizations of ZnTIA, CoTIA and CdTIA MOFs	S7- S9
Section S4. Stability of ZnTIA, CoTIA and CdTIA MOFs in Water:	S10-12
Section S5. BET Surface area and SEM images of ZnTIA, CoTIA and CdTIA MOFs	S13-S16
Section S6. Single crystal X-ray diffraction data collection, structure solution and refinement procedures.	S17- S28
Section S7. Single crystal structures.	S29-S35
Section S8. Powder pattern of vapour assisted aZnTIA, aCoTIA and aCdTIA	S36-S38
Section S9. Electrochemical measurements	S39
Section S10. Supplementary tables	S40-S44

S1: General Information:

General Remarks:

N, N-dimethylformamide (DMF), Thionyl chloride, hydrazine hydrate, benzene, ethanol, diethyl ether was purchased from Avra chemicals and 5-amino isophthalic acid were obtained from Sigma Aldrich Chemicals. All the chemicals and solvents were used without further purification. Solvothermal Experiment were performed in 5 mL culture tube inside a programmed oven for ZnTIA, CoTIA and CdTIA MOFs.

Instruments:

- ❖ **Fourier transform infrared (FT-IR) spectra:** Fourier transform infrared (FT-IR) spectra were taken on IRAffinity-1 (Shimadzu, Japan) spectrometer at Zn-Se ATR (attenuated total reflection) mode in the 4000-400 cm^{-1} (mid IR range) region.
- ❖ **Powder X-ray diffraction (PXRD):** Bruker D8 Advanced XRD (excitation source: 2.2KW Cu-anode ceramic tube) was used for analysing the PXRD pattern of all the MOFs. We have processed further the PXRD data by using the X'pert High Score Plus software for the background correction.
- ❖ **Thermogravimetric analyses (TGA):** Thermo-gravimetric analysis (TGA) was recorded over the temperature range between 25 to 800 °C on a SDT Q600 TG-DTA analyzer in the presence of N_2 atmosphere with heating rate of 20 °C min^{-1} .
- ❖ **Gas adsorption:** Adsorption isotherms were measured in Quantachrome USA device at 77 K (maintained by liquid N_2). Before analysis the MOFs samples were degassed for 12h at 100 °C in the presence of liquid nitrogen.
- ❖ **Scanning Electron Microscopy (SEM):** SEM (Scanning Electron Microscopy) was performed on Model No: EVO/18 Research Brand Name: Carl Zeiss.
- ❖ **Electrochemical Workstation:** All the electrochemical experiments were carried out in a standard three-electrode system where a glassy carbon electrode (GCE) was used as a substrate for the working

electrode, Hg/HgO was used as reference electrode and graphite rod was used as a counter electrode with an electrochemical workstation Autolab (PGSTAT204 - Metrohm-Autolab, Netherlands; 2015).

S2: Experimental Methodology:

S2.1: Synthesis of aZnTIA:

We synthesized aZnTIA following the reported procedure.^{S1a} Briefly, crystals of *p*ZnTIA (0.5mmol) were subjected to ball milling (containing 10 stainless steel balls inside) for 2h at 400 rpm under Ar atmosphere. The milling process consisted of 5 minutes of milling followed by a 5-minute pause. After the completion of the reaction, the product was extracted by gently scraping the inside surface of the stainless-steel jar, including both the walls and the balls. In addition, the sample underwent a degassing process for 6 hours at a temperature of 100 °C. Finally, the product was designated as aZnTIA.

S2.2: Synthesis of aCoTIA:

To synthesize aCoTIA, crystals of *p*CoTIA (0.5mmol) were subjected to ball milling (containing 10 stainless steel balls inside) for 2h at 400 rpm under Ar atmosphere. The milling process consisted of 5 minutes of milling followed by a 5-minute pause. After the completion of the reaction, the product was extracted by gently scraping the inside surface of the stainless-steel jar, including both the walls and the balls. In addition, the sample underwent a degassing process for 6 hours at a temperature of 100 °C. Finally, the product was designated as aCoTIA.

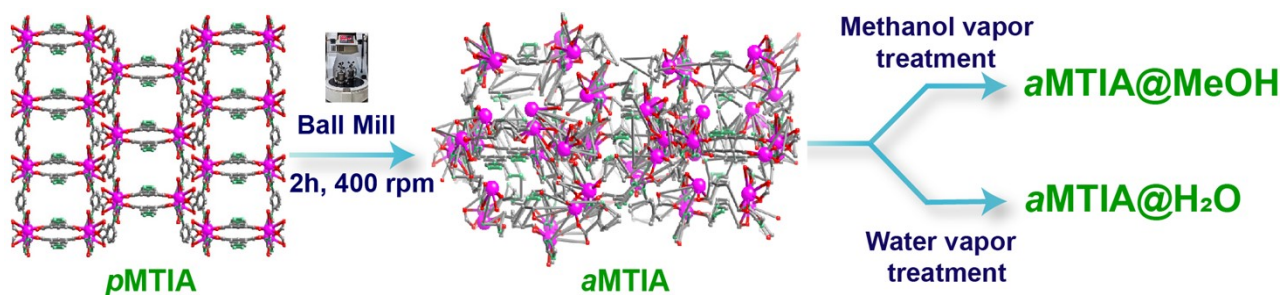
S2.3: Synthesis of aCdTIA:

To synthesize aCdTIA, crystals of *p*CdTIA (0.5mmol) were subjected to ball milling (containing 10 stainless steel balls inside) for 2h at 400 rpm under Ar atmosphere. The milling process consisted of 5 minutes of milling followed by a 5-minute pause. After the completion of the reaction, the product was extracted by gently scraping the inside surface of the stainless-steel jar, including both the walls and the balls. In addition, the sample underwent a degassing process for 6 hours at a temperature of 100 °C. Finally, the product was designated as aCdTIA.

S2.4: Mechanism of humidity-assisted crystallization of aZnTIA, aCoTIA and aCdTIA.

The humidity or water vapor exposure significantly influences the transformation of the amorphous structure caused by ball milling into a crystalline structure. Humidity serves as an external stimulus that helps to reconstruct the framework of order. However, the process of exposure to humidity occurred not only on the surface of the particles but also throughout the whole of the amorphous

state, although some regions may retain the amorphous state.^{S2a} We took 10mg of aZnTIA, aCoTIA and aCdTIA in different glass vials and kept them in different vapor conditions. 1st set of three vials was kept in methanol vapor for 78h at 25°C (aZnTIA@MeOH, aCoTIA@MeOH and aCdTIA@MeOH), and 2nd set of three vials was kept in 95% water vapor condition for 78h at 25°C (aZnTIA@H₂O, aCoTIA@H₂O and aCdTIA@H₂O). After completion of the reaction, all the vapor-treated samples were degassed properly for 48h at 100°C and further characterized through PXRD.



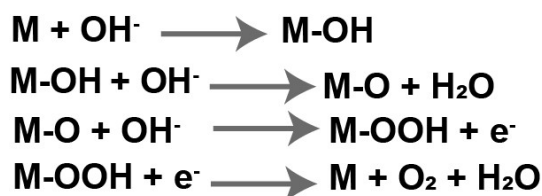
Scheme S1: Schematic presentation of synthesis of aMTIA from pMTIA and vapor exposure process to synthesis aMTIA@MeOH and aMTIA@H₂O [M- Zn(II), Co(II) and Cd (II), *p*- pristine state, *a*- amorphous state]. For a better understanding of the entire synthesis process, we choose pCoTIA framework.

S2.5: Mechanism of Oxygen Evolution Reaction in alkaline medium.

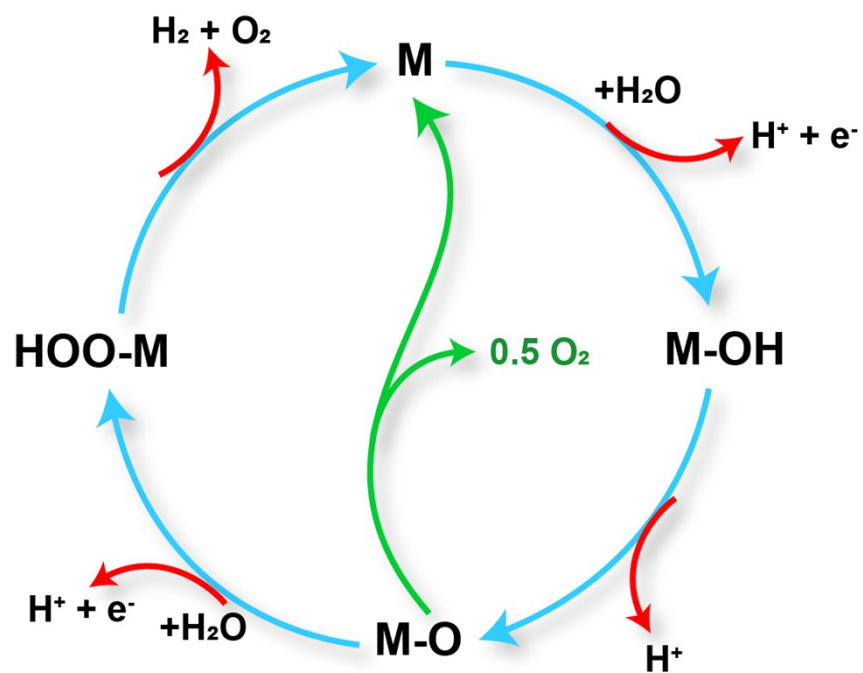
We carried out the oxygen evolution reaction in the alkaline medium (1M KOH). So, here is the mechanism as follows;



The overall OER catalytic ability is the bonding interactions with intermediates (e.g., M-OH, M-O, and M-OOH).



Where, M= electrocatalyst surface. Here evolution of oxygen occurred by formation of M-OOH intermediate.



Scheme S2: OER mechanism in alkaline conditions. The sky blue line indicates that the OER involves the formation of a peroxide (M–OH) intermediate, while the olive green line indicates the direct reaction of two adjacent oxo (M–O intermediates to produce oxygen.

S3: Characterizations of ZnTIA, CoTIA and CdTIA MOFs:

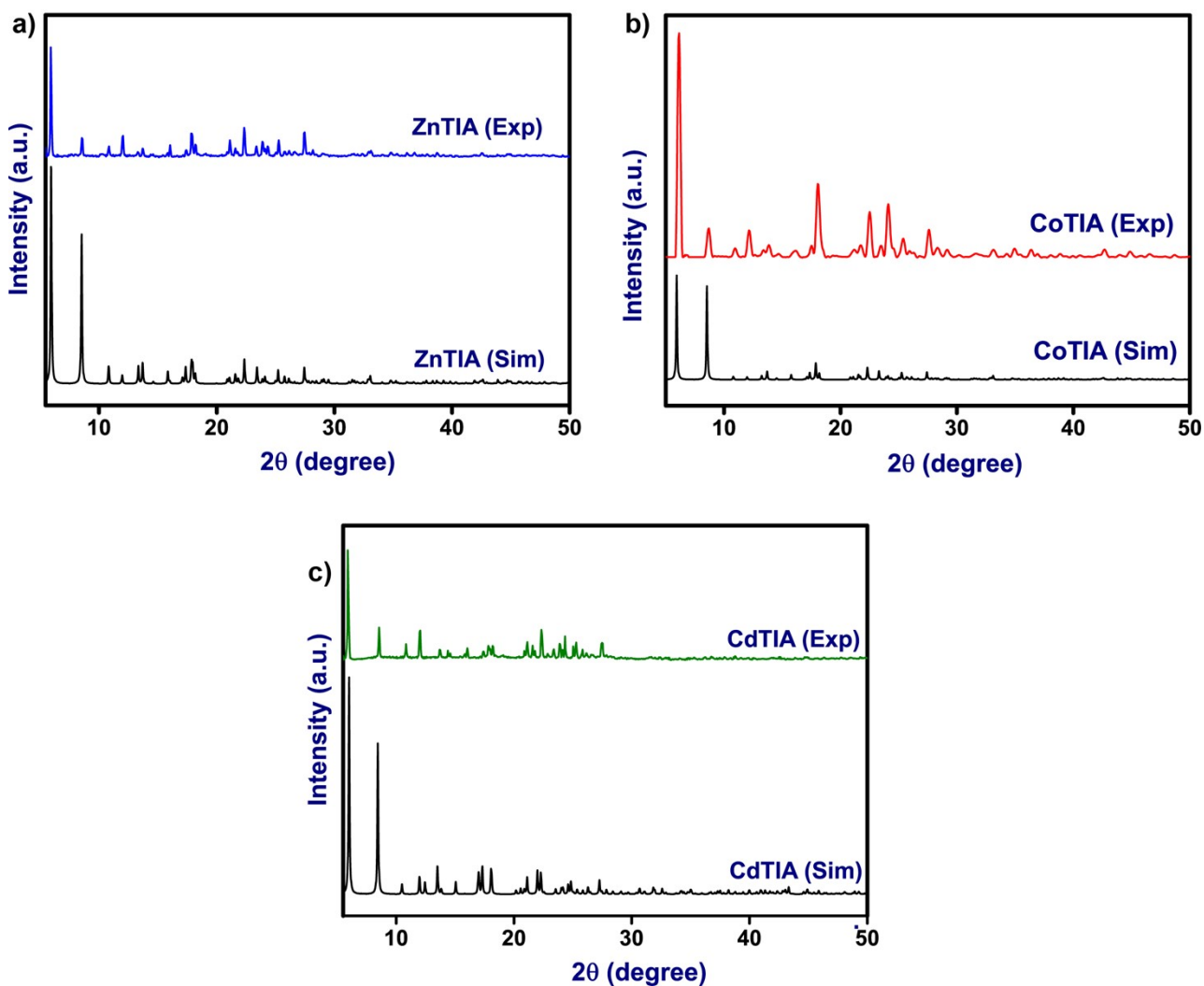


Figure S1: Experimental Powder XRD pattern (denoted as **Exp**) of a) ZnTIA (**blue**), b) CoTIA (**red**) and c) CdTIA (**olive green**), compared with simulated PXRD pattern (denoted as **Sim**) of ZnTIA (a, **black**), CoTIA (b, **black**) and CdTIA (c, **black**).

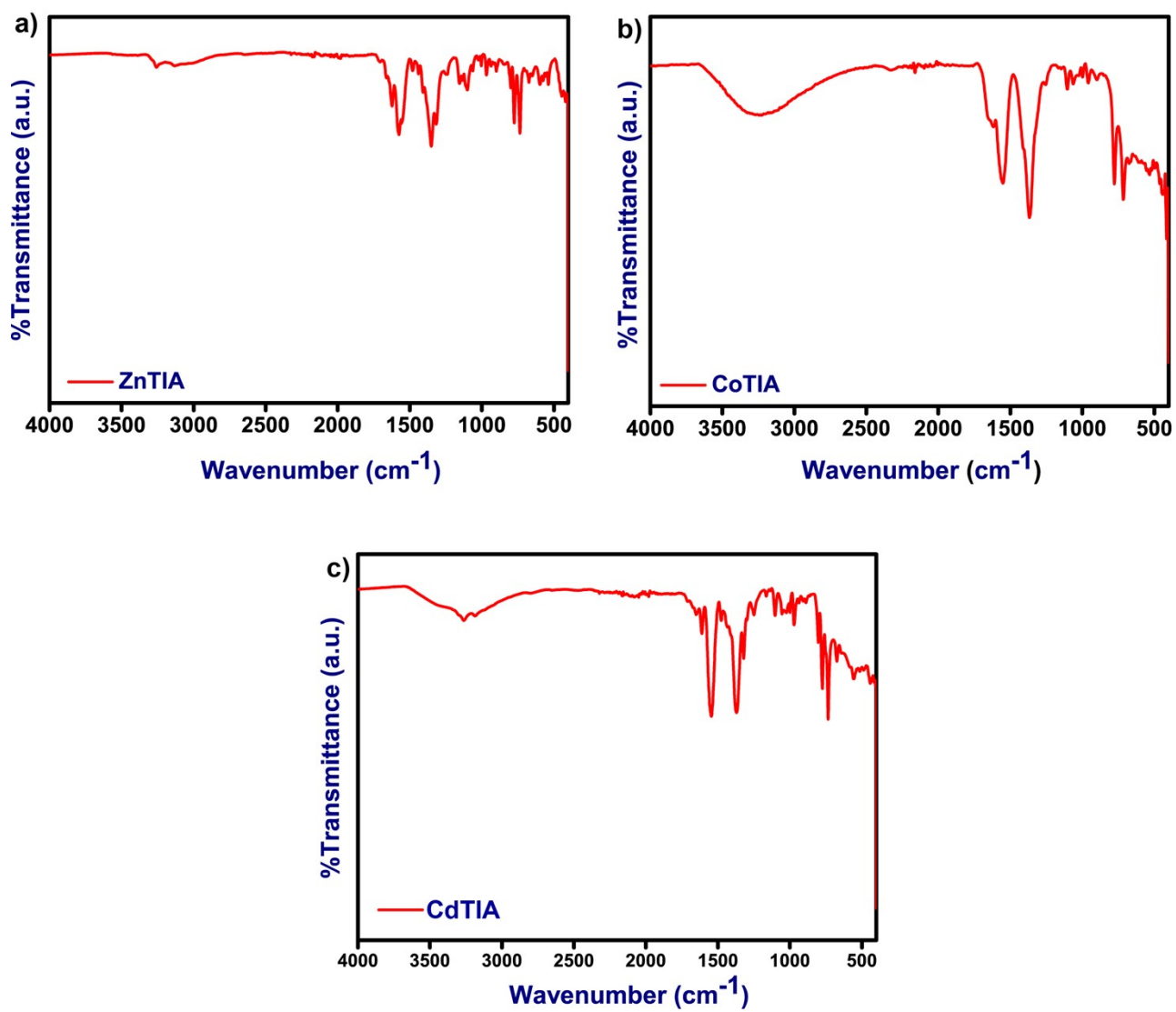


Figure S2: FT-IR analysis of a) ZnTIA, b) CoTIA and c) CdTIA MOFs.

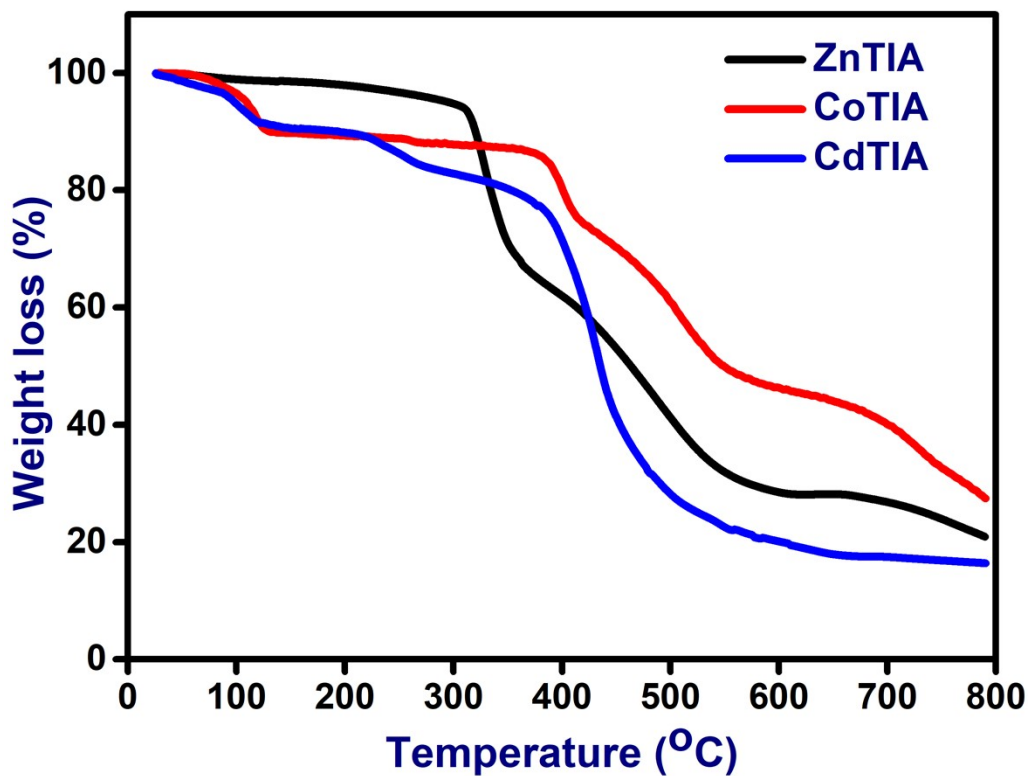


Figure S3: Thermogravimetric analysis of ZnTIA (black), CoTIA (red) and CdTIA (blue).

S4: Stability of ZnTIA, CoTIA and CdTIA MOFs in Water:

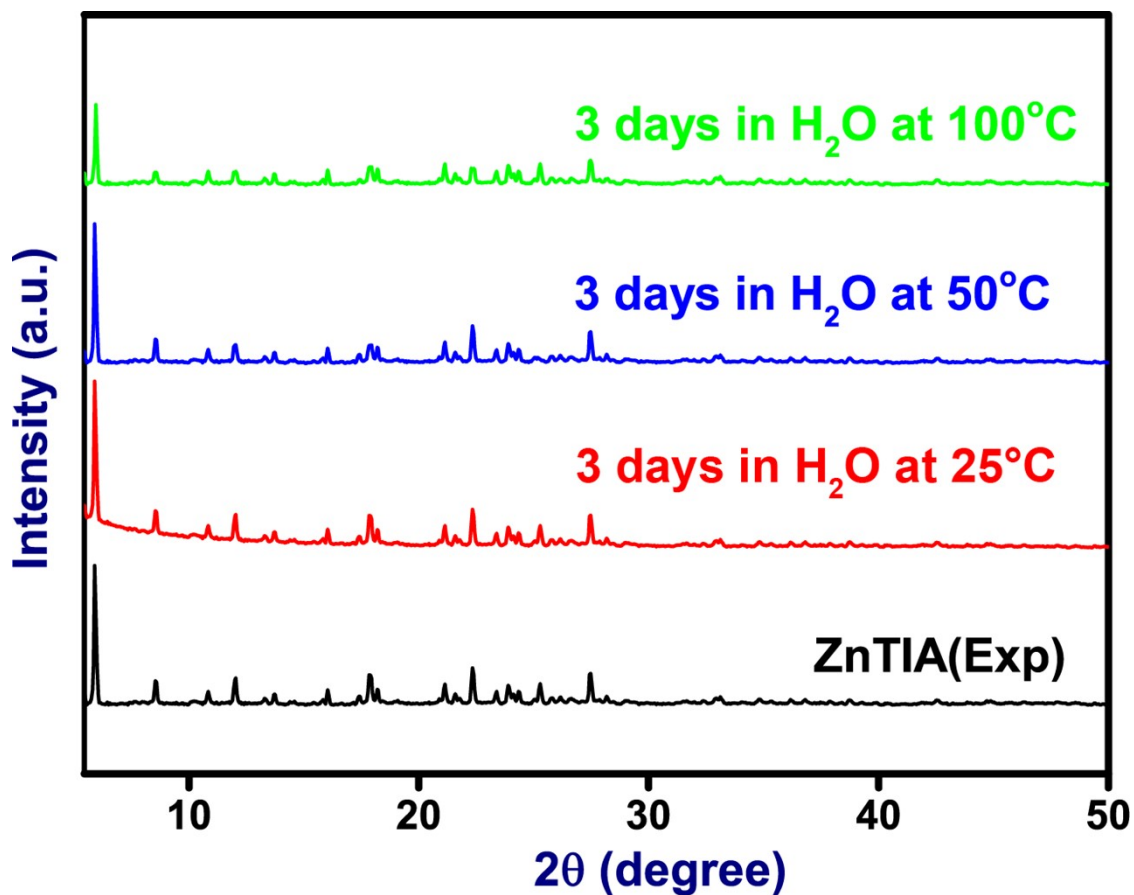


Figure S4: PXRD patterns of ZnTIA (Exp), performed during the stability test in water (at 25°C, 50°C and 100°C) for 3 days, The framework structure of all were unchanged after 3 days in water (25°C, 50°C) and boil water (100°C) for 3 days as evident from their sharp PXRD peak.

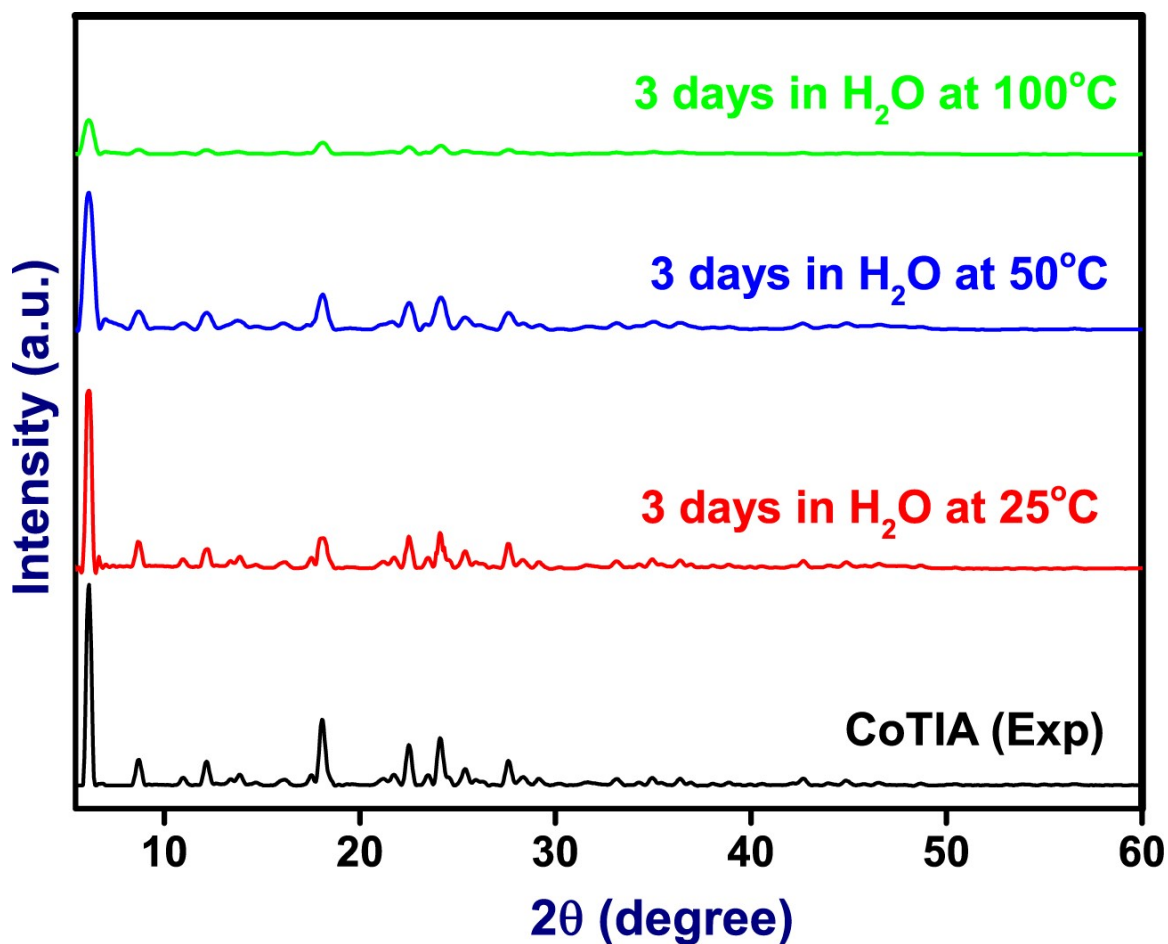


Figure S5: PXRD patterns of CoTIA (Exp), performed during the stability test in water (at 25°C, 50°C and 100°C) for 3 days, The framework structure of all were unchanged after 3 days in water (25°C, 50°C) and boil water (100°C) for 3 days as evident from their sharp PXRD peak.

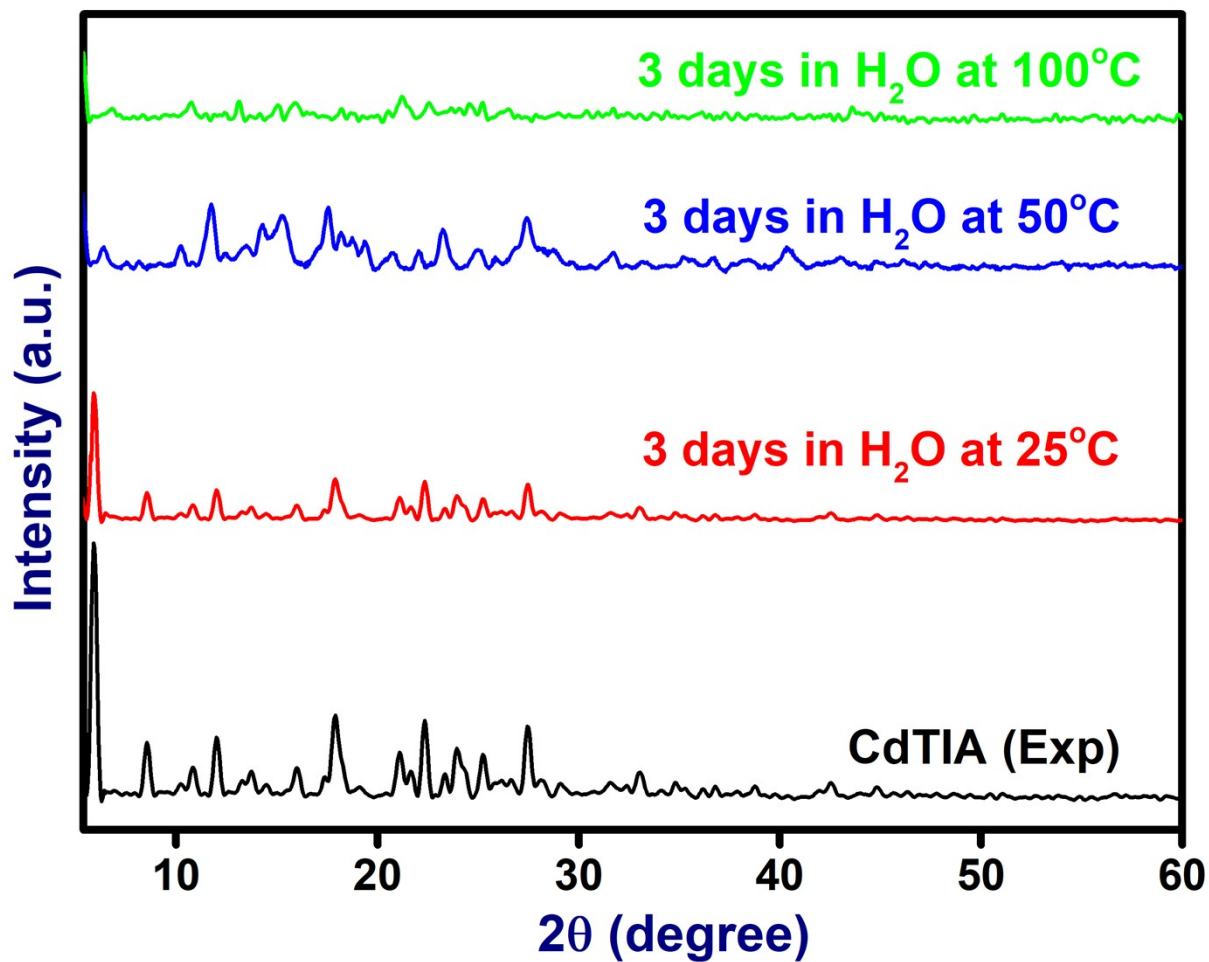


Figure S6: PXRD patterns of CdTIA (Exp), performed during the stability test in water (at 25°C, 50°C and 100°C) for 3 days, The framework structure of all were unchanged after 3 days in water (25°C, 50°C). But there is structural degradation in boiling water (100°C) for 3 days as evident from their sharp PXRD peak.

S5: BET Surface area and SEM images of ZnTIA, CoTIA and CdTIA MOFs:

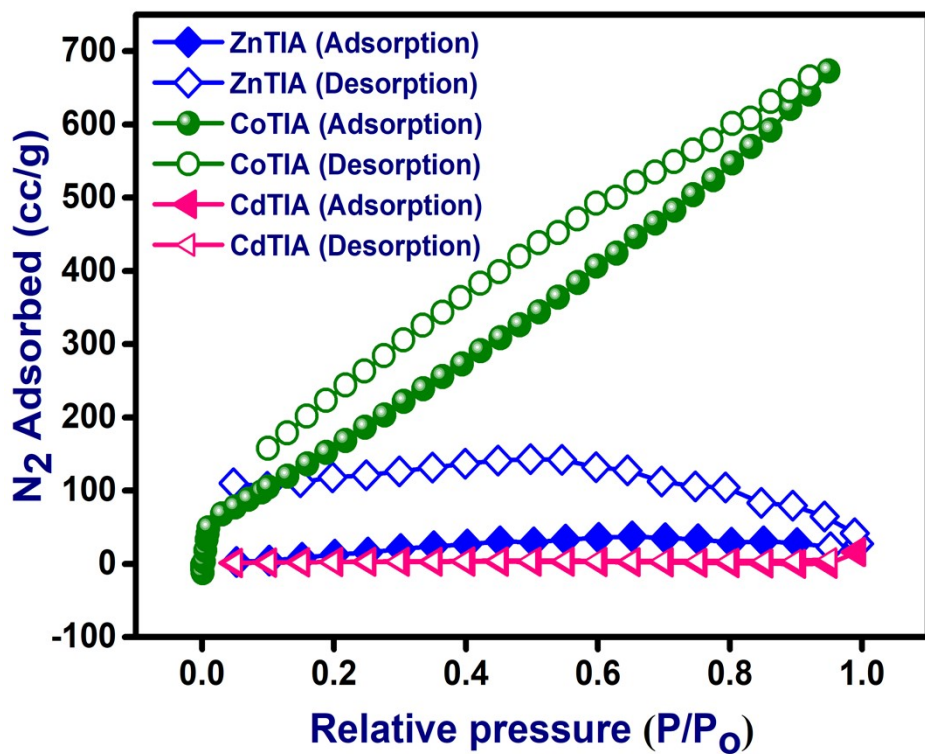


Figure S7a: N₂ gas adsorption isotherm of ZnTIA (blue), CoTIA (olive green) and CdTIA (pink).

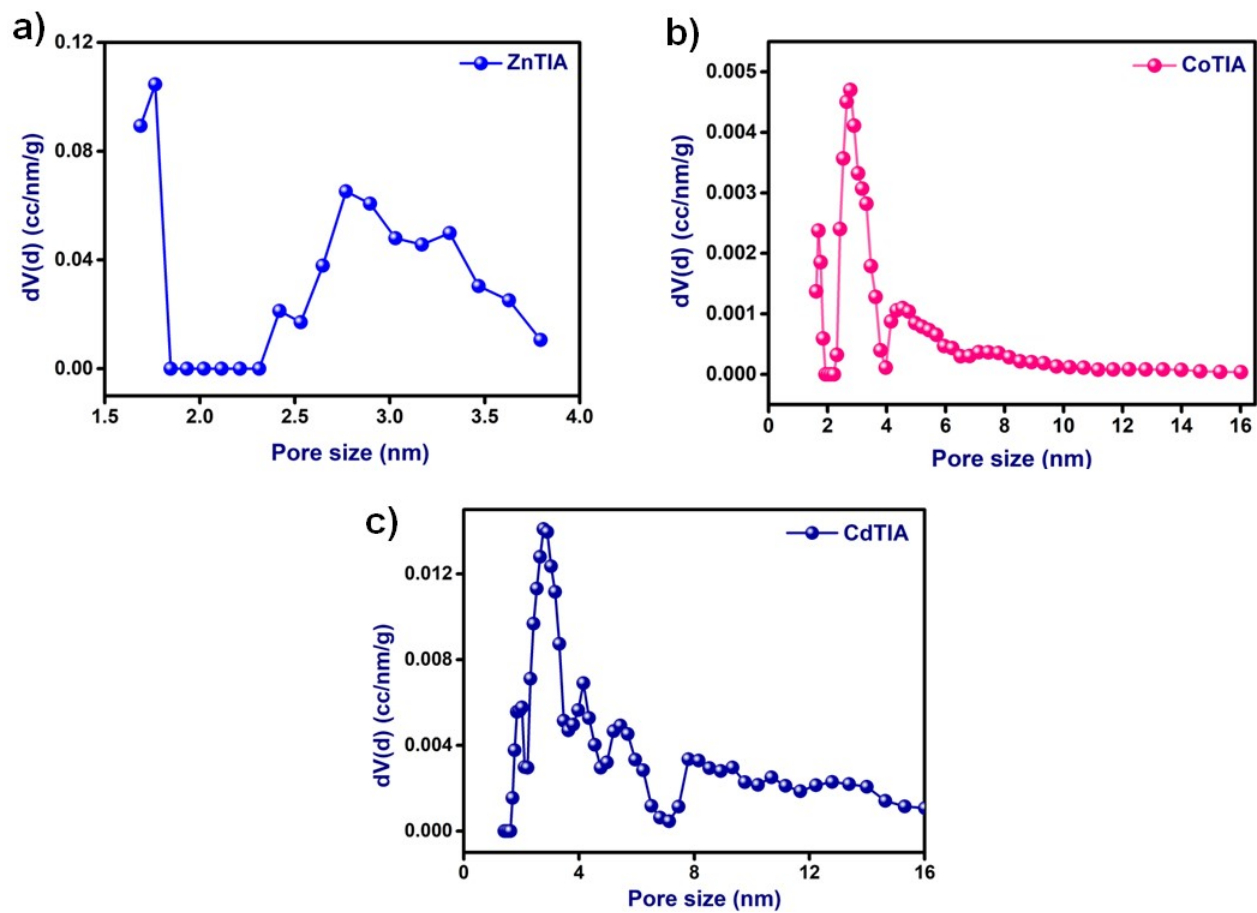


Figure S7b: The NLDFT pore size distribution of a) ZnTIA, b) CoTIA and c) CdTIA, measured from the nitrogen sorption data.

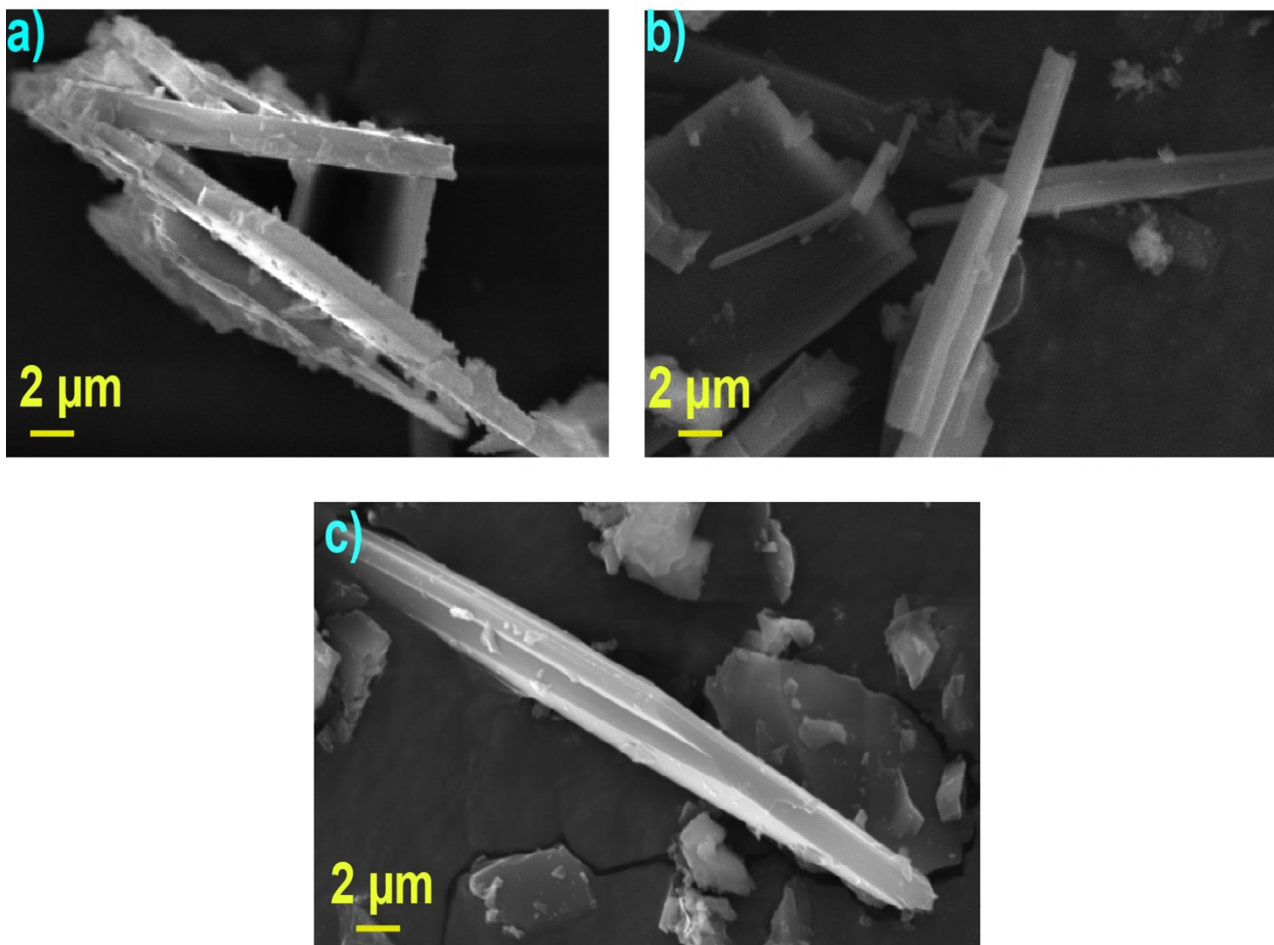
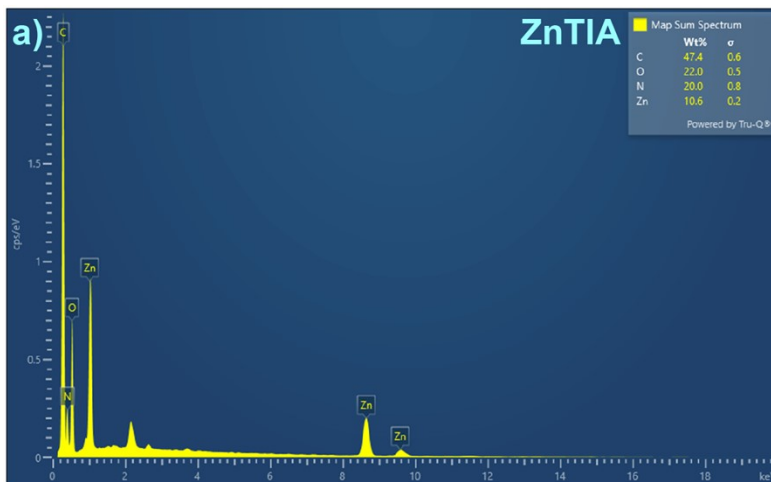
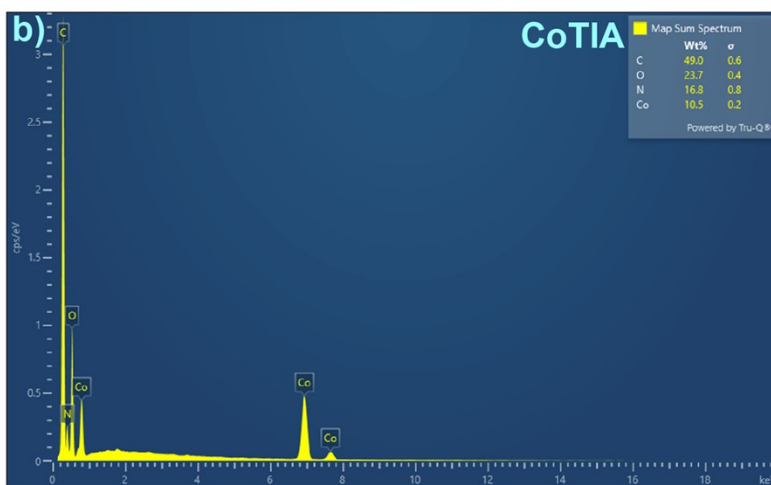


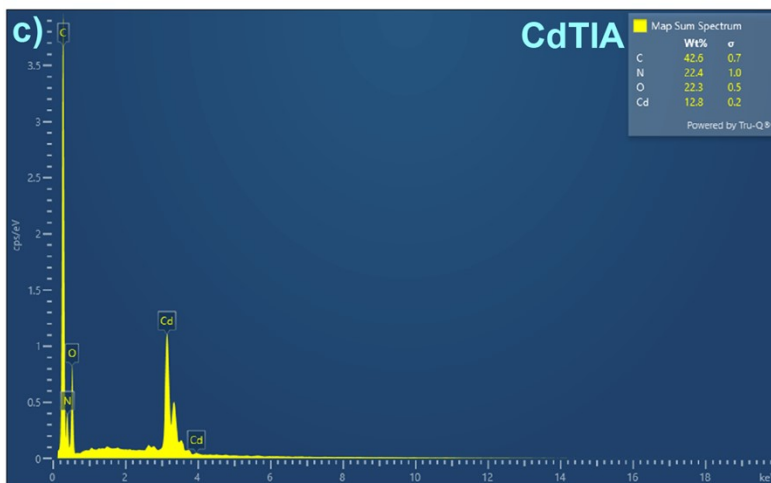
Figure S8a: SEM images of a) ZnTIA, b) CoTIA and c) CdTIA crystals.



	Wt%	σ
C	47.4	0.6
O	22.0	0.5
N	20.0	0.8
Zn	10.6	0.2



	Wt%	σ
C	49.0	0.6
O	23.7	0.4
N	16.8	0.8
Co	10.5	0.2



	Wt%	σ
C	42.6	0.7
O	22.3	0.5
N	22.4	1.0
Cd	12.8	0.2

Figure S8b: FESEM -EDAX of a) ZnTIA, b) CoTIA and c) CdTIA crystals.

Section S6. Single crystal X-ray diffraction data collection, structuresolution and refinement procedures.

General Data Collection and Refinement Procedures:

All single crystal data were collected on a Bruker SMART APEX three circle diffractometer equipped with a CCD area detector and operated at 1500 W power (50 kV, 30 mA) to generate Mo K α radiation ($\lambda=0.71073$ Å). The incident X-ray beam was focused and monochromated using Bruker Excalibur Gobel mirror optics. Crystals of the ZnTIA, CoTIA, and CdTIA reported in the paper were mounted on nylon CryoLoops (Hampton Research) with Paraton-N (Hampton Research).

Initial scans of each specimen were performed to obtain preliminary unit cell parameters and to assess the mosaicity (breadth of spots between frames) of the crystal to select the required frame width for data collection. In every case frame widths of 0.5° were judged to be appropriate and full hemispheres of data were collected using the *Bruker SMART*^{S3} software suite. Following data collection, reflections were sampled from all regions of the Ewald sphere to redetermine unit cell parameters for data integration and to check for rotational twinning using *CELL_NOW*^{S4}. In no data collection was evidence for crystal decay encountered. Following exhaustive review of the collected frames, the resolution of the dataset was judged. Data were integrated using *Bruker SAINT*^{S5} software with a narrow frame algorithm and a 0.400 fractional lower limit of average intensity. Data were subsequently corrected for absorption by the program *SADABS*^{S6}. The space group determinations and tests for merohedral twinning were carried out using *XPREP*^{S7}. In all cases, the highest possible space group was chosen.

All structures were solved by direct methods and refined using the *SHELXTL 97*^{S8} software suite. Atoms were located from iterative examination of difference F-maps following least squares refinements of the earlier models. Final models were refined anisotropically (if the number of data permitted) until full convergence was achieved. Data were collected at 293 K for ZnTIA, CdTIA and CoTIA presented in this paper. This lower temperature was considered to be optimal for obtaining the best data. Electron density within void spaces has not been assigned to any guest entity but has been modeled as isolated oxygen and/or carbon atoms. The foremost errors in all the models are thought to lie in the assignment of guest electron density. All structures were examined using the *Adsym* subroutine of *PLATON*^{S9} to assure that no additional symmetry could be applied to the models. All ellipsoids in ORTEP diagrams are displayed at the 50% probability level unless noted otherwise. For all structures we note that elevated R-values are commonly encountered in MOF crystallography for the reasons expressed above by us and by other research groups.^{S10-S19}

- S3. Bruker (2005). *APEX2*. Version 5.053. Bruker AXS Inc., Madison, Wisconsin, USA.
- S4. Sheldrick, G. M. (2004). *CELL_NOW*. University of Göttingen, Germany. Steiner, Th. (1998). *Acta Cryst.* B54, 456–463.
- S5. Bruker (2004). *SAINT-Plus* (Version 7.03). Bruker AXS Inc., Madison, Wisconsin, USA.
- S6. Sheldrick, G. M. (2002). *SADABS* (Version 2.03) and *TWINABS* (Version 1.02). University of Göttingen, Germany.
- S7. Sheldrick, G. M. (1997). *SHELXS '97* and *SHELXL '97*. University of Göttingen, Germany.
- S8. WINGX version 1.80.04. Louis Farrugia, University of Glasgow.
- S9. A. L. Spek (2005) *PLATON, A Multipurpose Crystallographic Tool*, Utrecht University, Utrecht, The Netherlands.
- S10. Dakin, L. A., Ong P. C., Panek, J. S., Staples, R. J. & Stavropoulos, P. *Organometallics* **19**, 2896-2908 (2000).
- S11. Noro, S., Kitaura, R., Kondo, M., Kitagawa, S., Ishii, T., Matsuzaka, H. & Yamashita, M. *J. Am. Chem. Soc.* **124**, 2568-2583 (2002).
- S12. Eddaoudi, M., Kim, J., Vodak, D., Sudik, A., Wachter, J., O'Keeffe, M. & Yaghi, O.M. *Proc. Natl. Acad. Sci. U.S.A.* **99**, 4900-4904 (2002).
- S13. Heintz, R. A., Zhao, H., Ouyang, X., Grandinetti, G., Cowen, J. & Dunbar, K. R. *Inorg. Chem.* **38**, 144-156 (1999).
- S14. Biradha, K., Hongo, Y. & Fujita, M. *Angew. Chem. Int. Ed.* **39**, 3843-3845 (2000).
- S15. Grosshans, P., Jouaiti, A., Hosseini, M. W. & Kyritsakas, N. *New J. Chem, (Nouv. J. Chim.)* **27**, 793-797 (2003).
- S16. Takeda, N., Umemoto, K., Yamaguchi, K. & Fujita, M. *Nature (London)* **398**, 794-796 (1999).
- S17. Eddaoudi, M., Kim, J., Rosi, N., Vodak, D., Wachter, J., O'Keeffe, M. & Yaghi, O.M. *Science* **295**, 469-472 (2002).
- S18. Kesanli, B., Cui, Y., Smith, M. R., Bittner, E. W., Bockrath, B. C. & Lin, W. *Angew.*

Chem. Int. Ed. **44**, 72-75 (2005).

S19. Cotton, F. A., Lin, C. & Murillo, C. A. *Inorg. Chem.* **40**, 478-484 (2001).

Single crystal X-ray diffraction data of ZnTIA

A colorless crystal ($0.32 \times 0.26 \times 0.16 \text{ mm}^3$) of ZnTIA was mounted on 0.7 mm diameter nylon CryoLoops (Hampton Research) with Paraton-N (Hampton Research). The loop was mounted on a SMART APEX three circle diffractometer equipped with a CCD area detector (Bruker Systems Inc., 1999a)¹⁹ and operated at 1500 W power (50 kV, 30 mA) to generate Mo K_α radiation ($\lambda=0.71073 \text{ \AA}$). The incident X-ray beam was focused and monochromated using Bruker Excalibur Gobel mirror optics. A total of 7345 reflections were collected of which 5916 were unique and 3509 of these were greater than $2\sigma(I)$. The range of θ was from $3.07 - 28.94^\circ$. Analysis of the data showed negligible decay during collection. The structure was solved in Orthorhombic *Cmc21* space group, with $Z = 4$, using direct methods. Final full-matrix least-squares refinement on F^2 converged to $R_1 = 0.0613$ and $wR_2 = 0.1589$ (all data) with GOF = 1.091. Table S1 contains crystallographic data for the ZnTIA (CCDC No: 2336784).

➤ Refine_special_details:

Alert Level A

PLAT411_ALERT_2_A The H2B is the hydrogen from ethanol solvent and H27 is the hydrogen from triazole moiety. The short interaction between H2B and H27 is due to the disorder present in the ethanol solvent molecule.

PLAT602_ALERT_2_A The crystal structure of ZnTIA exhibits a significant quantity of voids and has a very porous character. Thus, the particular A level Alert will be presented in this specific type of structure.

Table S1. Crystal data and structure refinement for ZnTIA

Empirical formula	C ₃₀ H ₁₅ N ₉ O ₁₂ Zn ₂ , 2(C ₂ H ₆ O)
Formula weight	916.43
Temperature	293 K
Wavelength	0.71073 Å
Crystal system	Orthorhombic
Space group	<i>Cmc</i> 21
Unit cell and dimension	$a = 29.8348(19)$ Å $\alpha = 90^\circ$ $b = 11.0642(4)$ Å $\beta = 90^\circ$ $c = 13.2894(5)$ Å $\gamma = 90^\circ$
Volume	4386.8 (4)
Z	4
Density (calculated)	1.388
Absorption coefficient	1.163
F(000)	1864
Crystal size	0.32 × 0.26 × 0.16 mm ³
Theta range for data collection	3.07 – 28.94
Index ranges	-24 ≤ h ≤ 40, -14 ≤ k ≤ 15, -15 ≤ l ≤ 18
Reflections collected	7345
Independent reflections	5916
Completeness to theta = 26.02°	99
Absorption correction	Semi-empirical from equivalents
Refinement method	Full-matrix least-squares on F ²
Data / restraints / parameters	5916 / 1 / 275
Goodness-of-fit on F²	1.091
Final R indices [$I > 2\sigma(I)$]	$R_1 = 0.0613$, $wR_2 = 0.1589$
R indices (all data)	$R_1 = 0.0780$, $wR_2 = 0.1720$
Largest diff. peak and hole	0.865 and -0.646 e.Å ⁻³

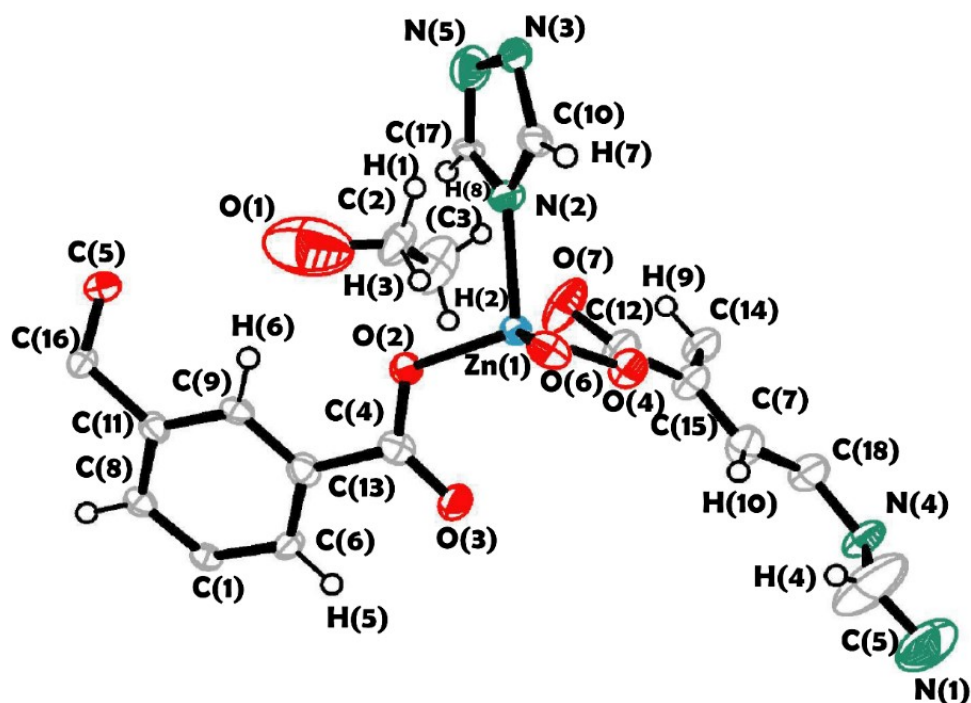


Figure S9: ORTEP diagram of the asymmetric unit of ZnTIA crystal.

Single crystal X-ray diffraction data of CoTIA

A pink crystal ($0.33 \times 0.27 \times 0.16 \text{ mm}^3$) of CoTIA was mounted on 0.7 mm diameter nylon CryoLoops (Hampton Research) with Paraton-N (Hampton Research). The loop was mounted on a *SMART APEX* three circle diffractometer equipped with a CCD area detector (Bruker Systems Inc., 1999a)¹⁹ and operated at 1500 W power (50 kV, 30 mA) to generate Mo K_{α} radiation ($\lambda=0.71073 \text{ \AA}$). The incident X-ray beam was focused and monochromated using Bruker Excalibur Gobel mirror optics. A total of 6377 reflections were collected of which 6100 were

unique and 3578 of these were greater than 2σ (I). The range of θ was from 3.05– 29.28°. Analysis of the data showed negligible decay during collection. The structure was solved in Orthorhombic *Cmc21*, with $Z = 4$, using direct methods. Final full matrix least-squares refinement on F^2 converged to $R_1 = 0.0659$ and $wR_2 = 0.1961$ (all data) with GOF = 1.090. Table S3 contains crystallographic data for the CoTIA (**CCDC No: 2336785**).

➤ **Refine_special_details:**

Alert Level A

PLAT415_ALERT_2_A The H12B is the hydrogen from ethanol solvent and H1A is the hydrogen from triazole moiety. The short interaction between H12B and H1A is due to the disorder present in the ethanol solvent molecule.

PLAT602_ALERT_2_A CoTIA crystal structures contain the large number of void space and are highly porous. Therefore, this type of A level Alert will come in this particular type of structure.

Table S2. Crystal data and structure refinement for CoTIA

Empirical formula	C ₃₀ H ₁₄ Co ₂ N ₉ O ₁₂ , 2(C ₂ H ₆ O)
Formula weight	903.51
Temperature	292 K
Wavelength	0.71073 Å
Crystal system	Orthorhombic
Space group	<i>Cmc21</i>
Unit cell and dimension	$a = 29.746(2)$ Å $\alpha = 90^\circ$ $b = 11.0402(7)$ Å $\beta = 90^\circ$ $c = 13.3648(7)$ Å $\gamma = 90^\circ$
Volume	4389.0(5)
Z	4
Density (calculated)	1.367
Absorption coefficient	0.826
F(000)	1840
Crystal size	0.33 × 0.27 × 0.16 mm ³
Theta range for data collection	3.05– 29.28
Index ranges	-40 ≤ h ≤ 40, -14 ≤ k ≤ 15, -16 ≤ l ≤ 18
Reflections collected	6377
Independent reflections	6100
Completeness to theta = 26.02°	99
Absorption correction	Semi-empirical from equivalents
Refinement method	Full-matrix least-squares on F ²
Data / restraints / parameters	6100 / 1 / 261
Goodness-of-fit on F²	1.090
Final R indices [$I > 2\sigma(I)$]	R ₁ = 0.0659, wR ₂ = 0.1961
R indices (all data)	R ₁ = 0.0771, wR ₂ = 0.2126
Largest diff. peak and hole	1.322 and -0.863 e.Å ⁻³

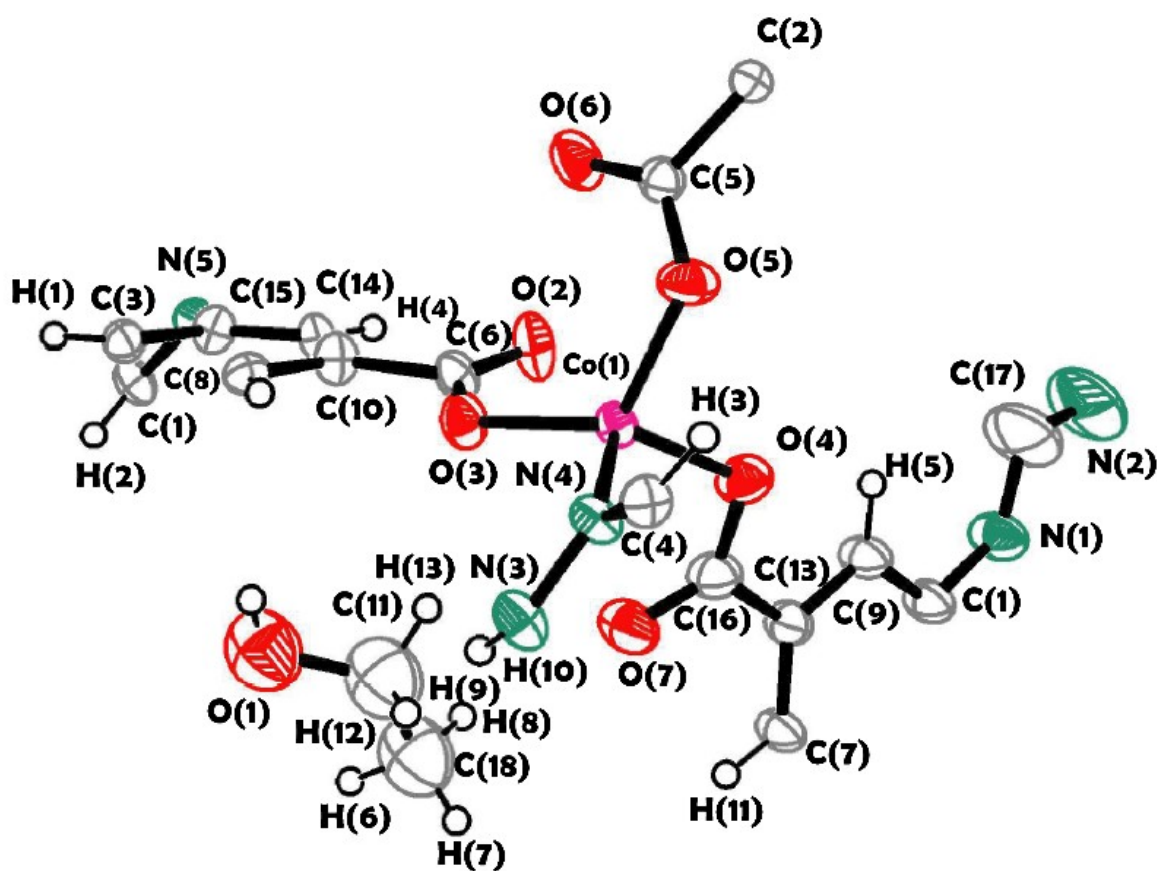


Figure S10: ORTEP diagram of the asymmetric unit of CoTIA crystal.

Single crystal X-ray diffraction data of CdTIA

A colorless type crystal ($0.30 \times 0.24 \times 0.17 \text{ mm}^3$) of CdTIA was mounted on 0.7 mm diameter nylon CryoLoops (Hampton Research) with Paraton-N (Hampton Research). The loop was mounted on a SMART APEX three circle diffractometer equipped with a CCD area detector (Bruker Systems Inc., 1999a)¹⁹ and operated at 1500 W power (50 kV, 30 mA) to generate Mo K_α radiation ($\lambda=0.71073 \text{ \AA}$). The incident X-ray beam was focused and monochromated using Bruker Excalibur Gobel mirror optics. A total of 6781 reflections were collected of which 6434 were unique and 4021 of these were greater than $2\sigma(I)$. The range of θ was from $3.11 - 29.14^\circ$. Analysis of the data showed negligible decay during collection. The structure was solved in Orthorhombic *Cmc21* space group, with $Z = 4$, using direct methods. Final full matrix least-squares refinement on F^2 converged to $R_1 = 0.0460$ and $wR_2 = 0.1293$ (all data) with GOF = 1.097. Table S2 contains crystallographic data for the CdTIA (CCDC No: 2336786).

➤ **Refine_special_details:**

PLAT602_ALERT_2_A CdTIA crystal structures contain the large number of void space and are highly porous. Therefore, this type of A level Alert will come in this particular type of structure.

Table S3. Crystal data and structure refinement for CdTIA

Empirical formula	C ₃₀ H ₁₄ Cd ₂ N ₉ O ₁₂ , 2(C ₂ H ₆ O)
Formula weight	1009.46
Temperature	293 K
Wavelength	0.71073 Å
Crystal system	Orthorhombic
Space group	<i>Cmc21</i>
Unit cell and dimension	$a = 29.4455(8) \text{ \AA}$ $\alpha = 90^\circ$ $b = 11.1947(3) \text{ \AA}$ $\beta = 90^\circ$ $c = 14.2083(3) \text{ \AA}$ $\gamma = 90^\circ$
Volume	4683.5(2)
Z	4
Density (calculated)	1.432
Absorption coefficient	0.974
F(000)	2004.0
Crystal size	0.30 × 0.24 × 0.17 mm ³
Theta range for data collection	3.11 – 29.14
Index ranges	-36 ≤ h ≤ 40, -8 ≤ k ≤ 15, -17 ≤ l ≤ 19
Reflections collected	6781
Independent reflections	6434
Completeness to theta = 26.02°	99
Absorption correction	Semi-empirical from equivalents
Refinement method	Full-matrix least-squares on F ²
Data / restraints / parameters	6434 / 1 / 270
Goodness-of-fit on F²	1.097
Final R indices [I > 2σ(I)]	R ₁ = 0.0460, wR ₂ = 0.1293
R indices (all data)	R ₁ = 0.0554, wR ₂ = 0.1381
Largest diff. peak and hole	0.929 and -0.491 e.Å ⁻³

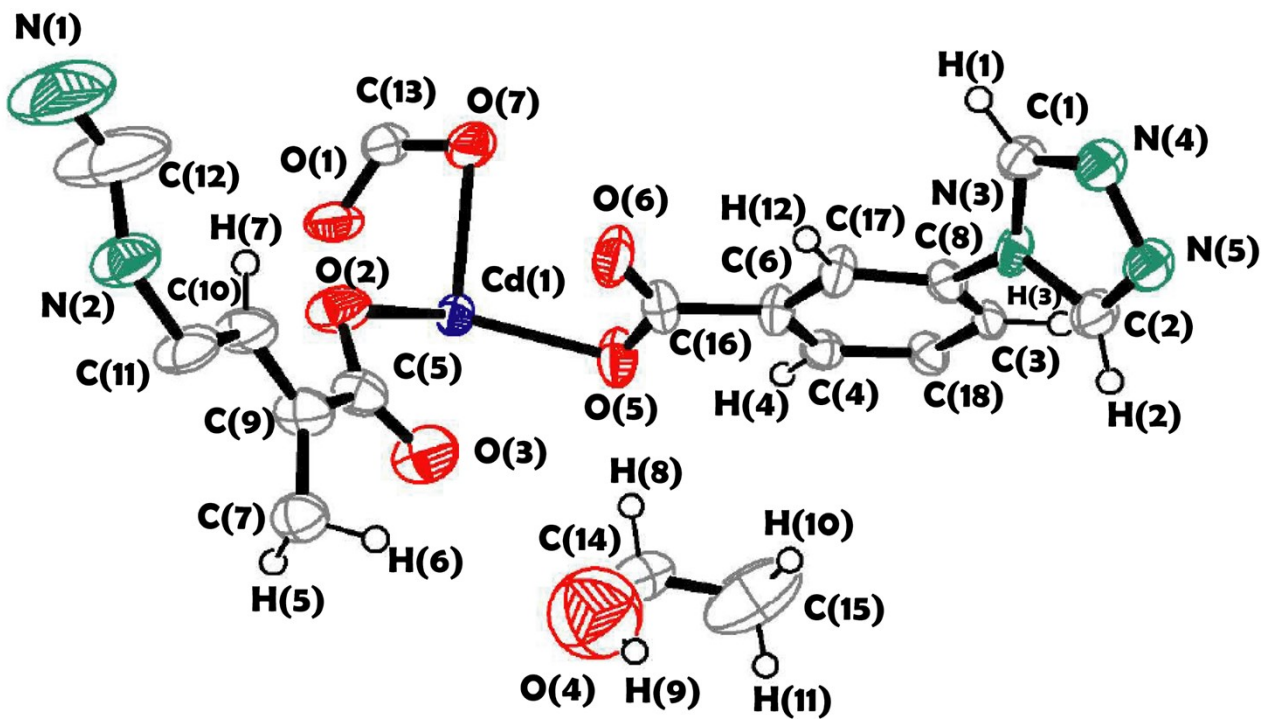


Figure S11: ORTEP diagram of the asymmetric unit of CdTIA crystal.

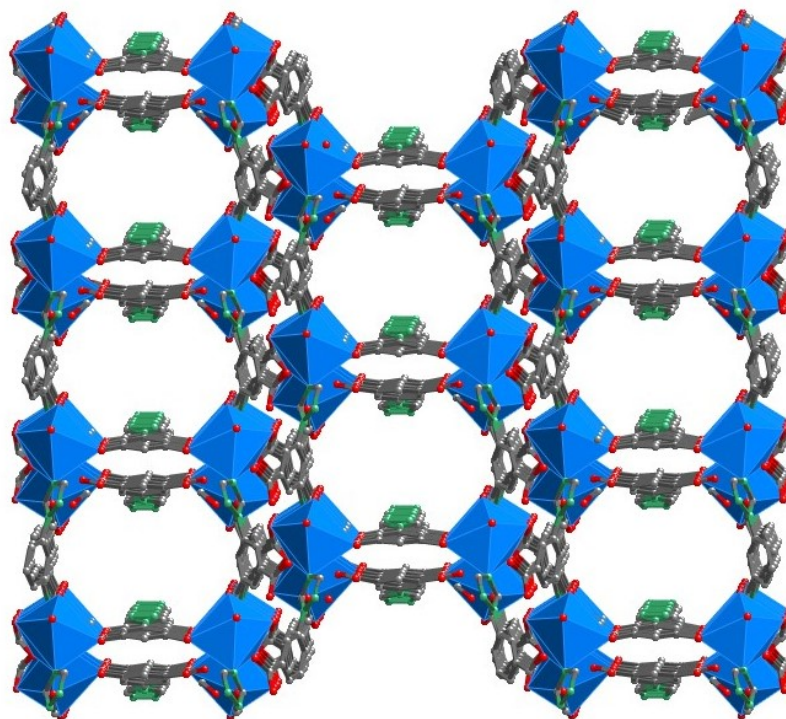


Figure S13: Packing diagram of ZnTIA, showing two-dimensional pores. Hydrogen atoms are omitted for clarity. Color code: Zn (II) (sky blue), N (olive green), O (red), C (grey).

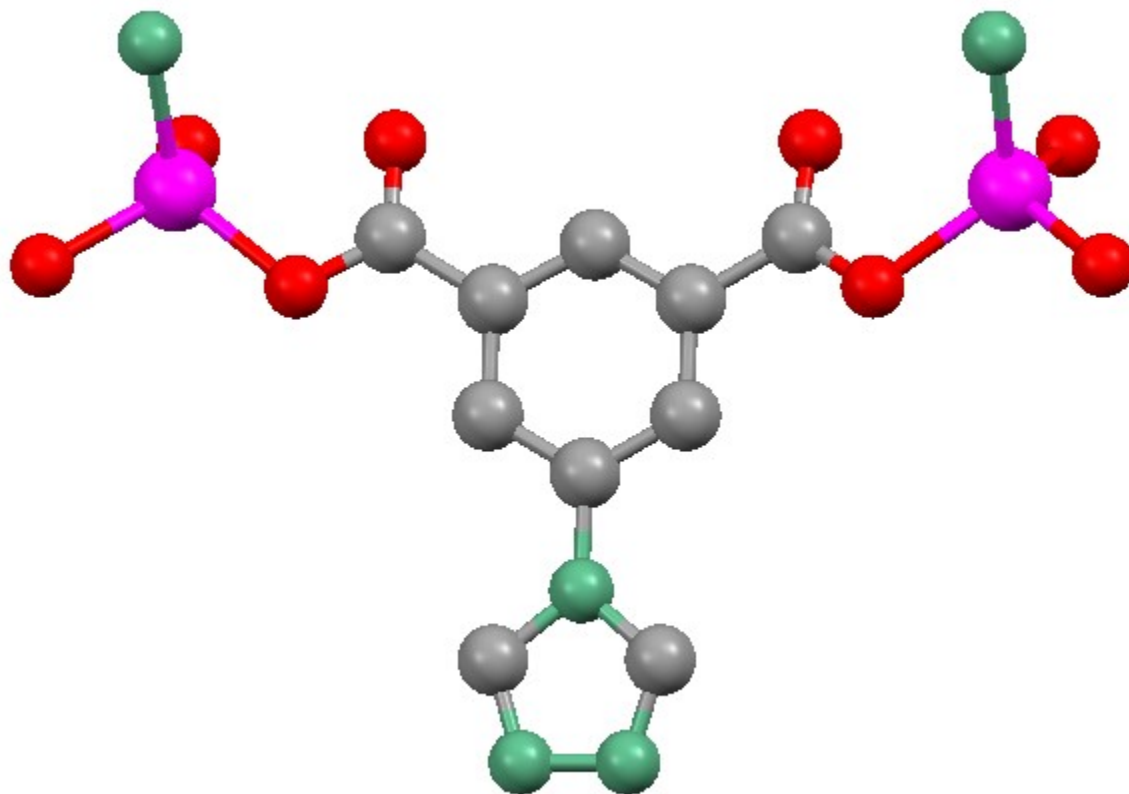


Figure S14: Crystal structure of CoTIA in ball and stick model. The coordination environment of Co(II) metal centre shown here. Hydrogen atoms are omitted here for clarity. Color code: Co (II) (Magenta), N (olive green), O (red), C (grey).

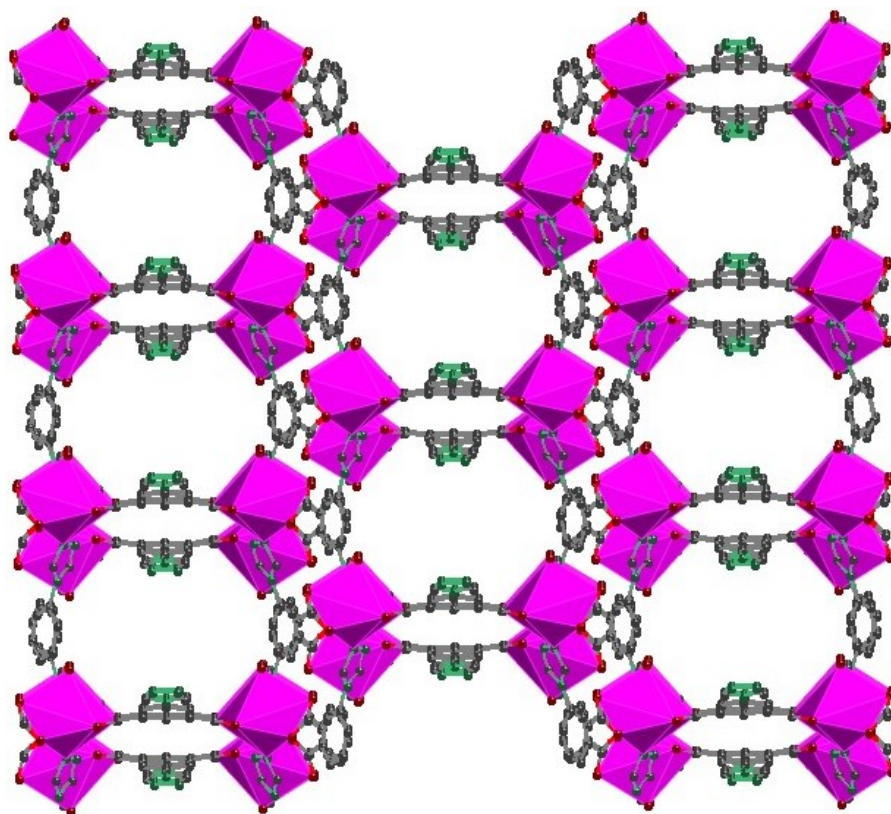


Figure S15: Packing diagram of CoTIA, showing two-dimensional pores. Hydrogen atoms are omitted for clarity. Color code: Co (II) (Magenta), N (olive green), O (red), C (grey).

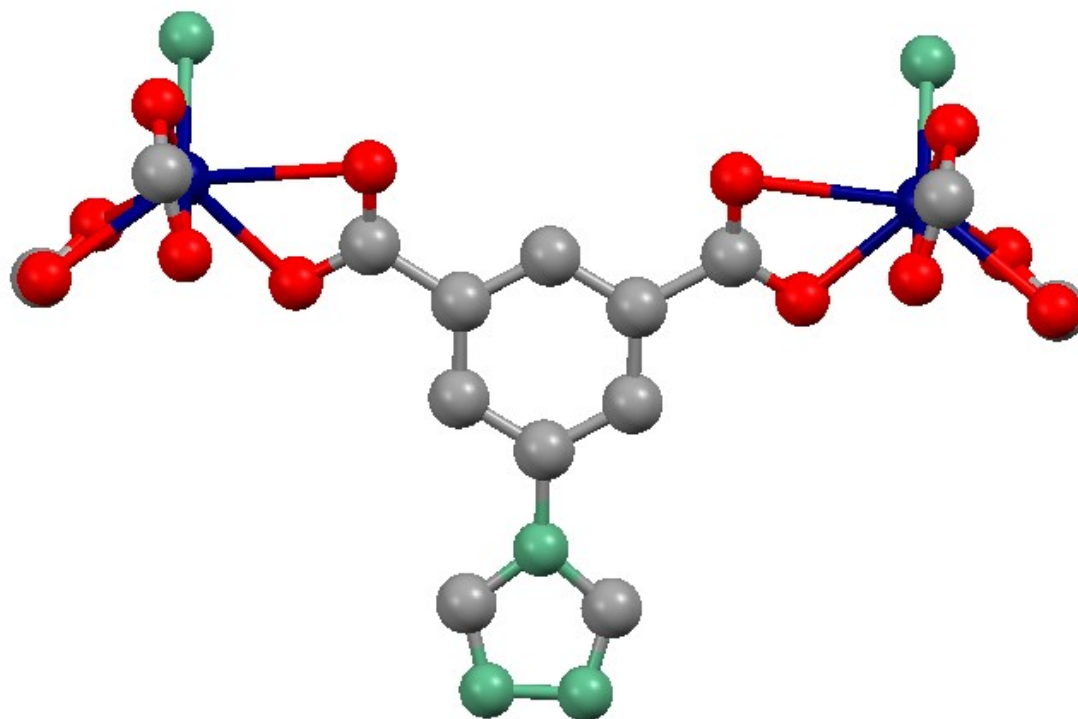


Figure S16: Crystal structure of CdTIA in ball and stick model. The coordination environment of Cd(II) metal centre shown here. Hydrogen atoms are omitted here for clarity. Color code: Cd (II) (**Indigo**), N (**olive green**), O (**red**), C (**grey**).

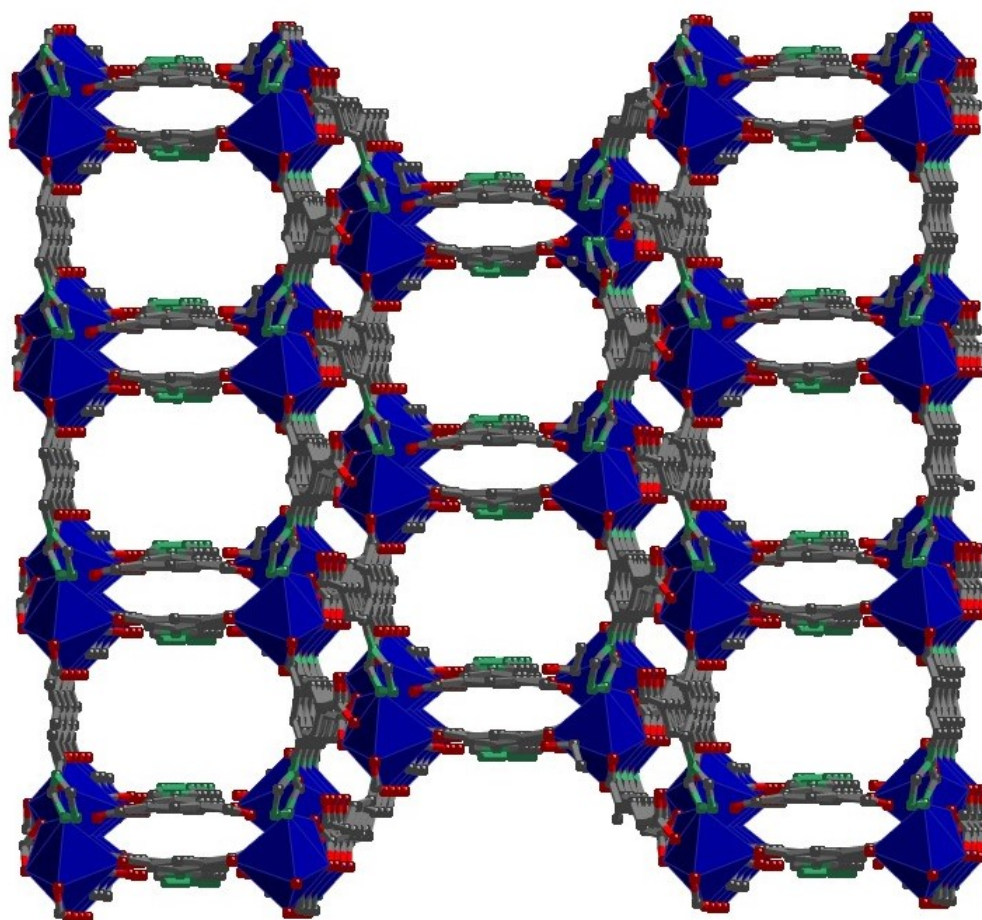


Figure S17: Packing diagram of CdTIA, showing two-dimensional pores. Hydrogen atoms are omitted for clarity. Color code: Cd (II) (**Indigo**), N (**olive green**), O (**red**), C (**grey**).

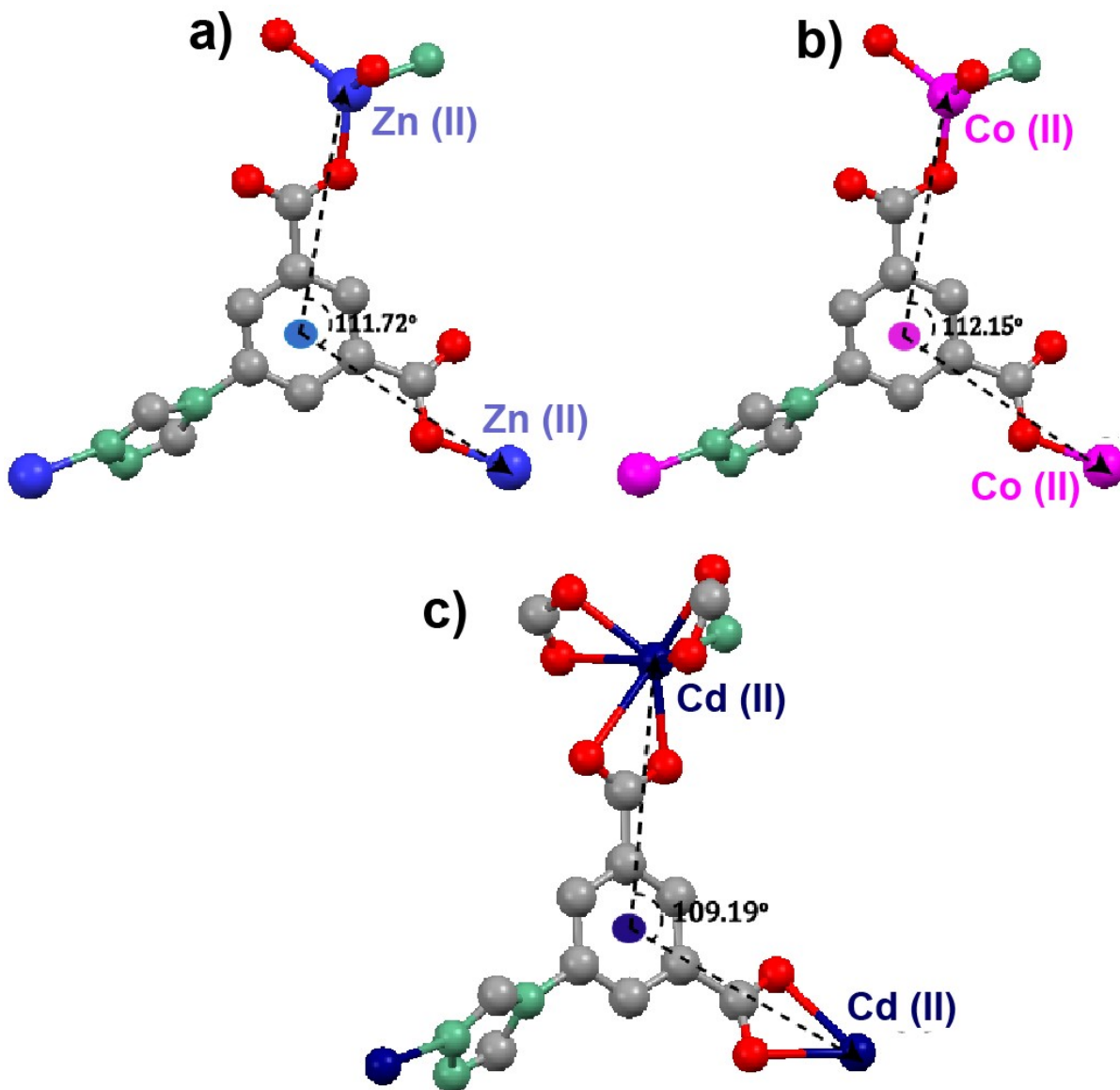


Figure S18: M-5-TIA-M angle, where 5-TIA coordinated via two -CO_2^- groups of two distinct a) Zn (II) [$\angle \text{Zn-5-TIA-Zn} = 111.72^\circ$], b) Co (II) [$\angle \text{Co-5-TIA-Co} = 112.15^\circ$], and c) Cd (II) [$\angle \text{Cd-5-TIA-Cd} = 109.19^\circ$] metal. Color code: Zn (II) (sky blue), Co (II) (magenta), Cd (II) (indigo), N (olive green), O (red), C (grey).

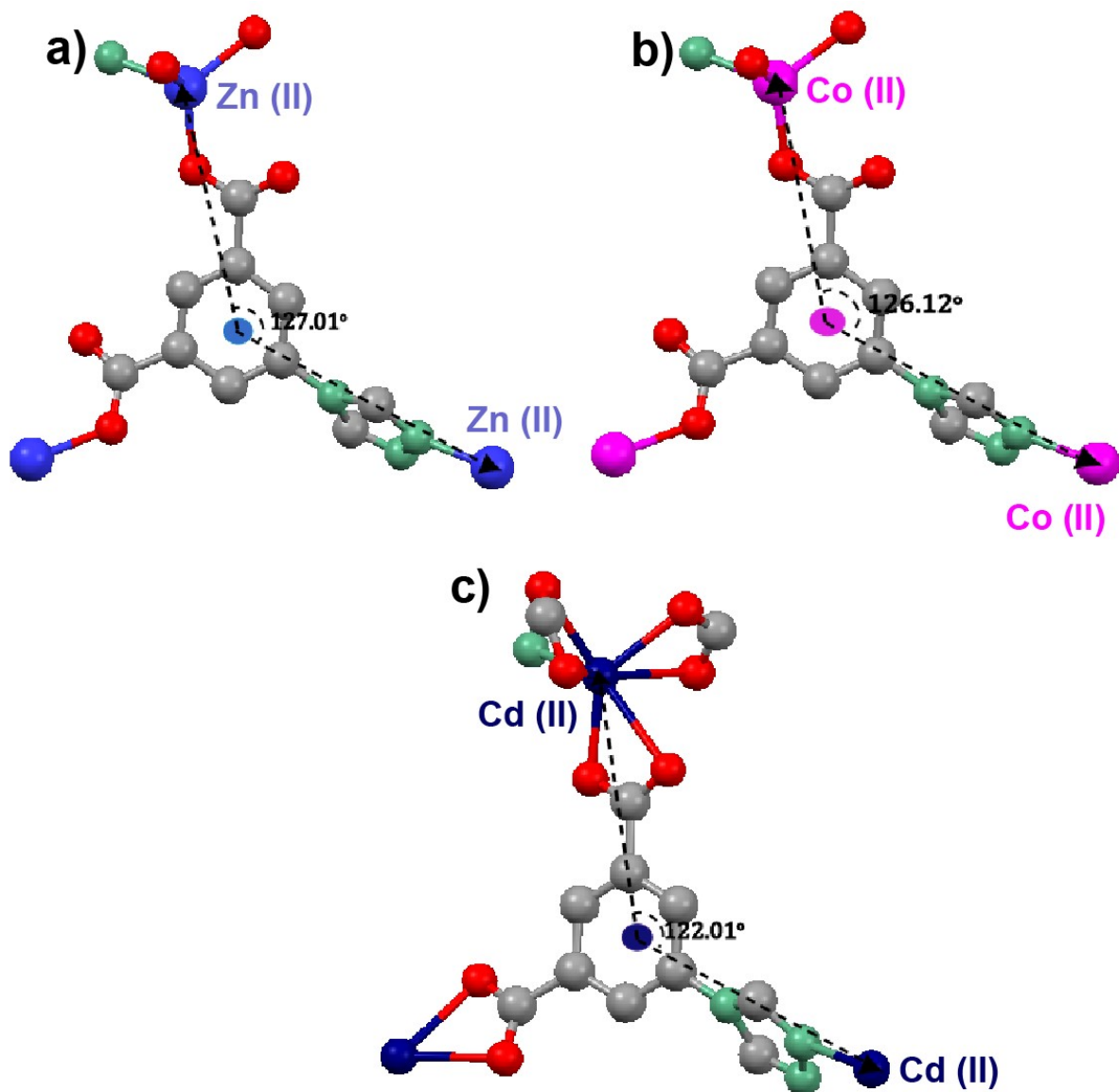


Figure S19: M-5-TIA-M angle, where 5-TIA coordinated via the one -CO_2^- and one μ_1 -triazolyl a) Zn (II) [$\angle \text{Zn-5-TIA-Zn} = 127.01^\circ$], b) Co (II) [$\angle \text{Co-5-TIA-Co} = 126.12^\circ$], and c) Cd (II) [$\angle \text{Cd-5-TIA-Cd} = 122.01^\circ$] metal. Color code: Zn (II) (sky blue), Co (II) (magenta), Cd (II) (indigo), N (olive green), O (red), C (grey).

S8: Powder pattern of vapour assisted aZnTIA, aCoTIA and aCdTIA:

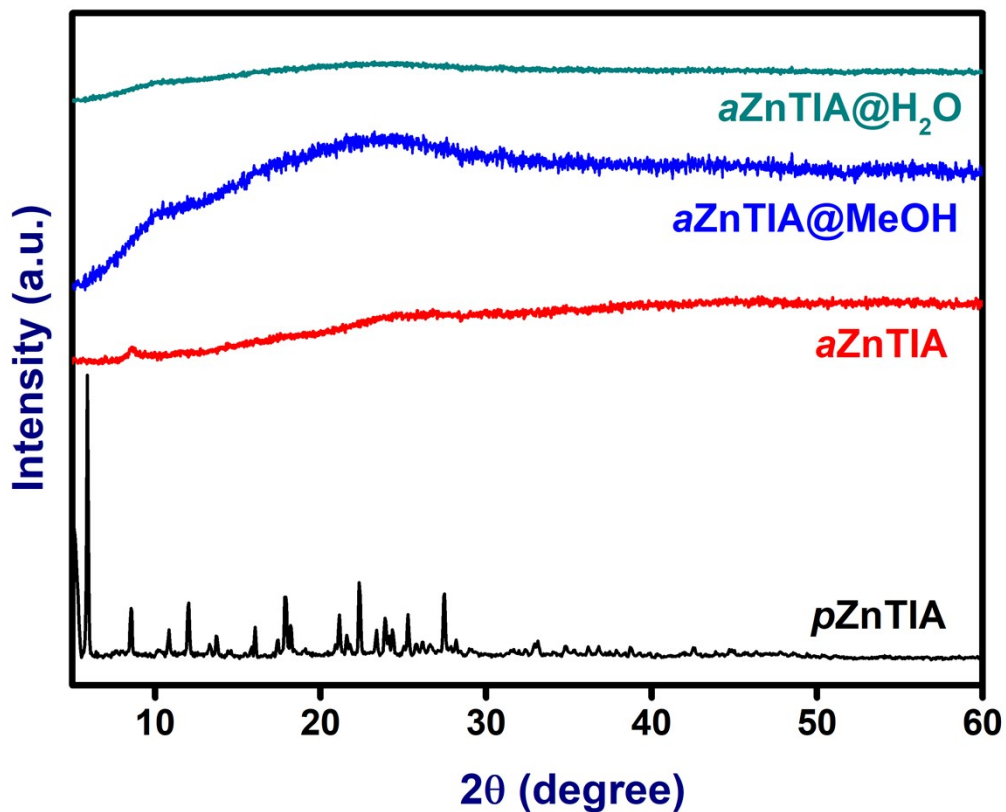


Figure S20: PXRD pattern of solvothermally synthesized crystal of *p*ZnTIA (**black**) compared with powder pattern of ball mill treated amorphous ZnTIA (*a*ZnTIA, **red**), methanol vapor treated *a*ZnTIA (*a*ZnTIA@MeOH, **blue**) and water vapor treated *a*ZnTIA (*a*ZnTIA@H₂O, **Persian green**). From the PXRD pattern, it confirmed that the *p*ZnTIA unable to tolerate the ball mill-induced mechanical force and not suitable candidate for alloy mixing process.

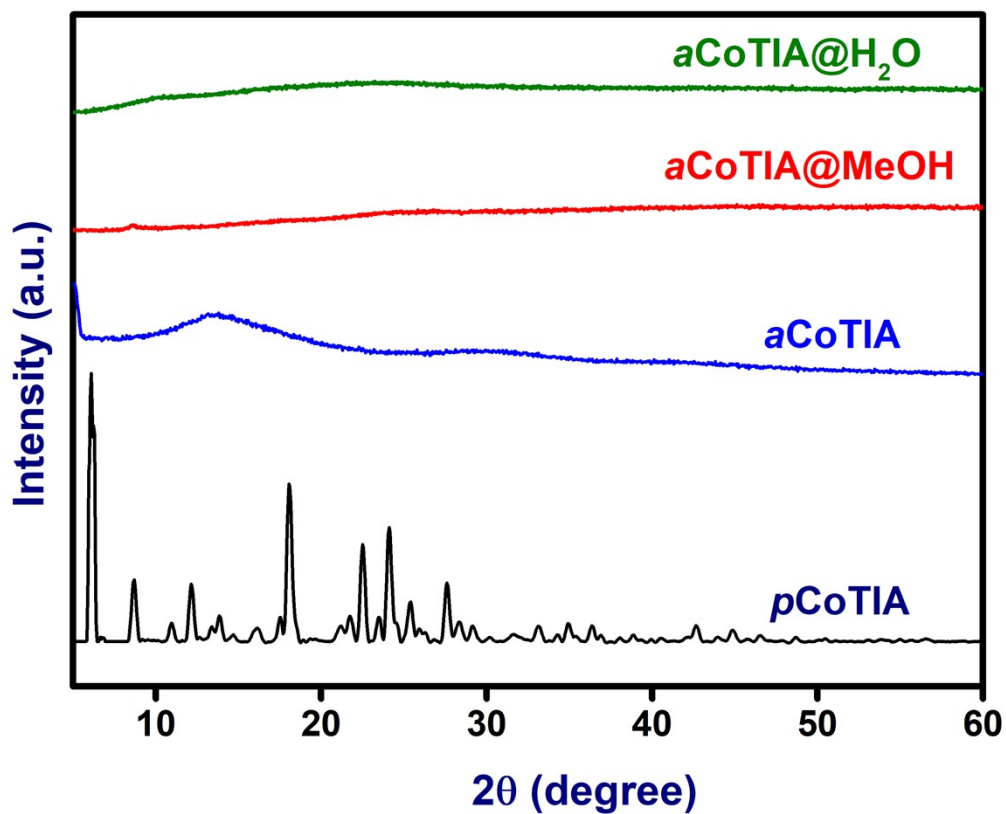


Figure S21: PXRD pattern of solvothermally synthesized crystal of *p*CoTIA (**black**) compared with powder pattern of ball mill treated amorphous CoTIA (*a*CoTIA, **blue**), methanol vapor treated *a*CoTIA (*a*CoTIA@MeOH, **red**) and water vapor treated *a*CoTIA (*a*CoTIA@H₂O, **olive green**). From the PXRD pattern, confirmed that the *p*CoTIA unable to tolerate the ball mill-induced mechanical force and not suitable candidate for alloy mixing process.

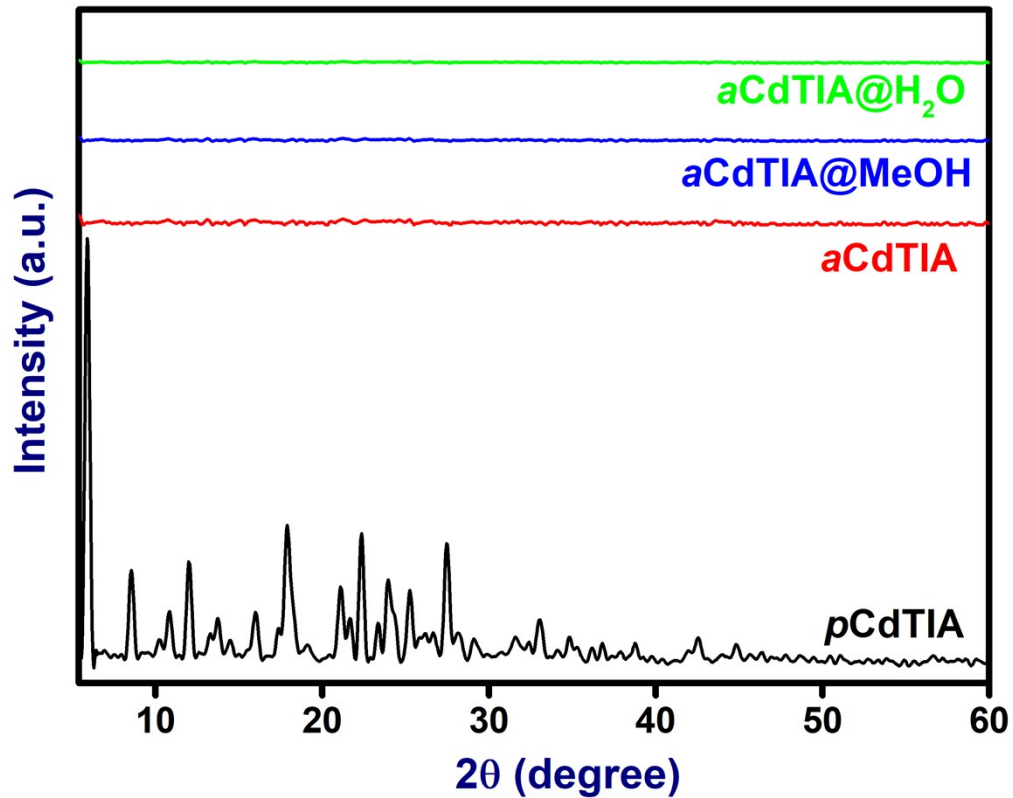


Figure S22: PXRD pattern of solvothermally synthesized crystal of *p*CdTIA (**black**) compared with powder pattern of ball mill treated amorphous CdTIA (*a*CdTIA, **red**), methanol vapor treated *a*CdTIA (*a*CdTIA@MeOH, **blue**) and water vapor treated *a*CoTIA (*a*CdTIA@H₂O, **magenta**). The PXRD pattern confirmed that the *p*CdTIA unable to tolerate the ball mill-induced mechanical force and not a suitable candidate for the alloy mixing process.

S9: Electrochemical Measurements:

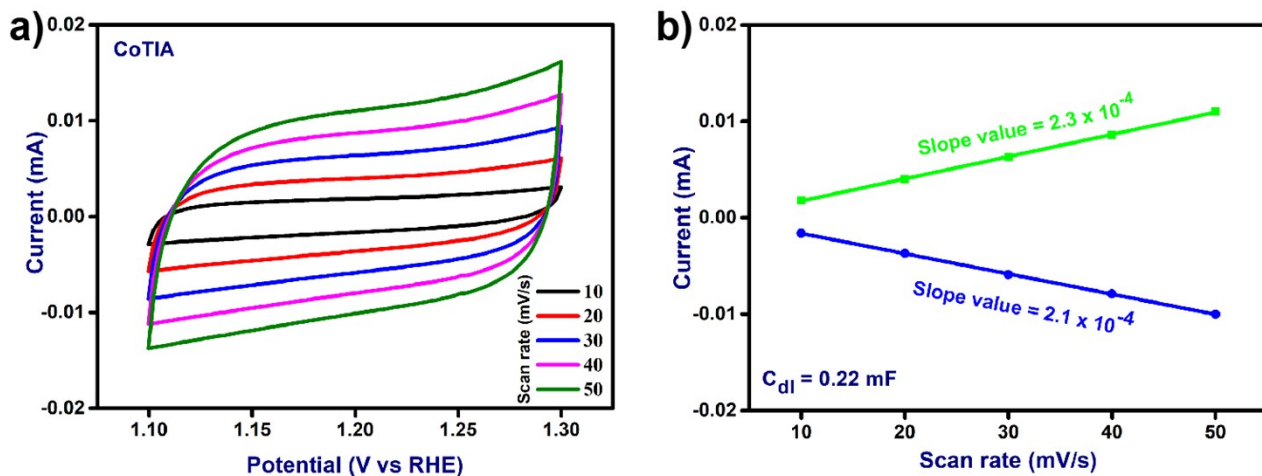


Figure S23: Cyclic voltammetry (CV) cycles at different scan rates from 10 to 50 mV s^{-1} in 1M KOH for (a) CoTIA, Corresponding anodic and cathodic current slope from the CV curves of (b) CoTIA.

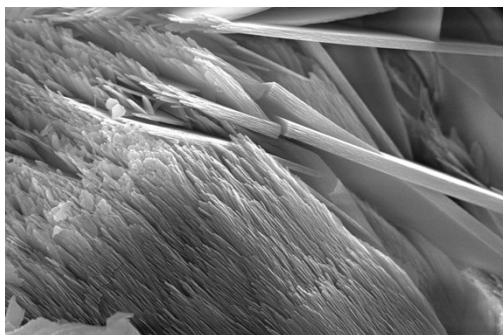


Figure S24: SEM image of CoTIA after the chronoamperometry test.

S10: Supplementary Tables:

Table S4: Attempt to synthesize the MOFs crystals of Zn(II), Co(II) and Cd(II) metal salts with TIA by various conditions in solvothermal synthesis:

SI No.	Solvents	Temp. (°C)	Product Formation
1.	DMF (N,N dimethyl formamide + NMP(N- methyl-2-pyrrolidone) (1:1))	120 °C and 90 °C	no product formed
2.	DMF: EtOH (1:1)	90 °C, 120 °C and 100 °C	Crystals of starting organic linker
3.	DMF : MeOH (2:1) and (1:1)	120 °C, 90 °C and 110 °C	Clear solution
4.	DMF + H ₂ O (1:1) and (2:1)	90 °C , 120 °C and 100 °C	Precipitate of unreacted precursor
5.	DEF (N,N diethylformamide) :MeOH	120 °C	Crystals of starting organic linker
6.	DEF: NMP	120 °C	Clear solution
7.	DEF: EtOH	120 °C	Clear solution
8.	DMF: EtOH (2:1) (This work)	120 °C	Crystals.

Table S5: . Types of Structure Directing Agents Used to Synthesize Crystals of ZnTIA, CoTIA and CdTIA.

SI No	Type of SDA	No Reaction	Unreacted starting material	Crystals of ZnTIA, CoTIA and CdTIA
1	$\begin{array}{c} \text{C}_4\text{H}_9 \text{---} \text{N}^{\oplus} \text{---} \text{C}_4\text{H}_9 \\ \text{C}_4\text{H}_9 \text{---} \text{N}^{\ominus} \text{---} \text{C}_4\text{H}_9 \\ \text{OH} \end{array}$	✓		
2	$\begin{array}{c} \text{C}_4\text{H}_9 \text{---} \text{N}^{\oplus} \text{---} \text{C}_4\text{H}_9 \\ \text{C}_4\text{H}_9 \text{---} \text{N}^{\ominus} \text{---} \text{C}_4\text{H}_9 \\ \text{Br} \end{array}$		✓	
3	$\begin{array}{c} \text{C}_2\text{H}_5 \text{---} \text{N}^{\oplus} \text{---} \text{C}_2\text{H}_5 \\ \text{C}_2\text{H}_5 \text{---} \text{N}^{\ominus} \text{---} \text{C}_2\text{H}_5 \\ \text{OH} \end{array}$		✓	
4	$\begin{array}{c} \text{C}_2\text{H}_5 \text{---} \text{N}^{\oplus} \text{---} \text{C}_2\text{H}_5 \\ \text{C}_2\text{H}_5 \text{---} \text{N}^{\ominus} \text{---} \text{C}_2\text{H}_5 \\ \text{Br} \end{array}$	✓		
5	$\begin{array}{c} \text{C}_2\text{H}_5 \text{---} \text{N}^{\oplus} \text{---} \text{C}_2\text{H}_5 \\ \text{C}_2\text{H}_5 \text{---} \text{N}^{\ominus} \text{---} \text{C}_2\text{H}_5 \\ \text{Cl} \end{array}$	✓		
5	$\begin{array}{c} \text{H}_3\text{C} \text{---} \text{N}^{\oplus} \text{---} \text{CH}_3 \\ \text{H}_3\text{C} \text{---} \text{N}^{\ominus} \text{---} \text{CH}_3 \\ \text{OH} \end{array}$		✓	
7	$\begin{array}{c} \text{H}_3\text{C} \text{---} \text{N}^{\oplus} \text{---} \text{CH}_3 \\ \text{H}_3\text{C} \text{---} \text{N}^{\ominus} \text{---} \text{CH}_3 \\ \text{Cl} \end{array}$			✓

Table S6: . The solvent/ solvent mixture used for vapor treatment on aMTIA [a-amorphous state; M= Zn, Co and Cd] to obtain the crystallinity back from the amorphous state.

SI No.	The solvent/ solvent mixture used for vapor treatment on aMTIA [a-amorphous state; M= Zn(II), Co(II) and Cd(II)]	Product Formation
1.	Methanol (MeOH)	Amorphous Product
2.	Water	Amorphous Product
3.	Diethyl ether	Amorphous Product
4.	Dichloromethane (DCM)	Amorphous Product
5.	Hexane	Amorphous Product
6.	Ethanol (EtOH)	Amorphous Product
7.	Acetone	Amorphous Product
8.	Acetonitrile	Amorphous Product
9.	Tetrahydrofuran (THF)	Amorphous Product
10.	Chloroform	Amorphous Product
11.	MeOH : EtOH (1:1)	Amorphous Product
12.	THF : Chloroform (1:1)	Amorphous Product

Table S7: Comparison table of reported MOF-based electrocatalysts with CoTIA towards OER activity

Electrocatalyst	Tafel slope (mV/dec)	Overpotential at (η^{10})	Electrolyte	References
CoTIA-1 mc	55.4	289	1M KOH	<i>Inorg. Chem</i> 2023 , 62 (8), 3457-3463.
NiCoS/Ti ₃ C ₂ T _x	58.2	365	1M KOH	<i>ACS Appl. Mater. Interfaces</i> , 2018, 10 , 22311–22319.
CoTIA	68.9	337	1M KOH	This work
Ni _{0.6} Co _{1.4} P	80	300	1M KOH	<i>Adv. Funct. Mater.</i> , 2018, 28 , 1–9.
Co-WOC-1	128	390	0.1 M KOH	<i>Angew. Chemie. Int. Ed.</i> , 2016, 55 , 2425–2430.
Co/ β -Mo ₂ C@N- CNTs	67	356	1M KOH	<i>Angew. Chemie. Int. Ed.</i> , 2019, 58 , 4923–4928.
Co/Co ₃ O ₄ @PGS	76.1	350	1M KOH	<i>Adv. Energy Mater.</i> , 2018, 8 , 1–11.

References:

S1a. Panda, T.; Horike, S.; Hagi, K.; Ogiwara, N.; Kadota, K.; Itakura, T.; Tsujimoto, M.; Kitagawa, S. *Angew. Chem. Int. Ed.* 2017, **56** (9), 2413-2417.

S2a. Benjamin, J. S.; Volin, T. E. *Metall. Trans.* 1974, **5** (8), 1929-1934.